

Supramolecular Construction of Cyanide-Bridged Re^I Diimine Multichromophores

Kristina S. Kisel,^{†,‡} Alexei S. Melnikov,[§] Elena V. Grachova,[†] Antti J. Karttunen,^{*,||} Antonio Doménech-Carbó,^{⊥,||} Kirill Yu. Monakhov,^{#,||} Valentin G. Semenov,[†] Sergey P. Tunik,[†] and Igor O. Koshevoy^{*,‡,||}

[†]Institute of Chemistry, St. Petersburg State University, Universitetskii pr. 26, Petergof, St. Petersburg 198504, Russia

[‡]Department of Chemistry, University of Eastern Finland, 80101 Joensuu, Finland

[§]Peter the Great St. Petersburg Polytechnic University, Polytechnicheskaya, 29, St. Petersburg 195251, Russia

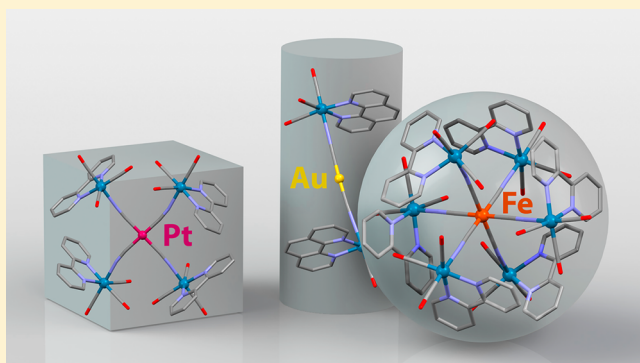
^{||}Department of Chemistry and Materials Science, Aalto University, 00076 Aalto, Finland

[⊥]Universidad de Valencia, Dr. Moliner 50, 46100 Burjassot, Valencia Spain

[#]Leibniz Institute of Surface Engineering (IOM), Permoserstraße 15, 04318 Leipzig, Germany

Supporting Information

ABSTRACT: The reactions of labile [Re(diimine)-(CO)₃(H₂O)]⁺ precursors (diimine = 2,2'-bipyridine, bpy; 1,10-phenanthroline, phen) with dicyanoargentate anion produce the dirhenium cyanide-bridged compounds [{Re(diimine)(CO)₃}₂CN]⁺ (**1** and **2**). Substitution of the axial carbonyl ligands in **2** for triphenylphosphine gives the derivative [{Re(phen)(CO)₂(PPh₃)₂CN]⁺ (**3**), while the employment of a neutral metalloligand [Au(PPh₃)(CN)] affords heterobimetallic complex [{Re(phen)(CO)₃NCu(PPh₃)]⁺ (**4**). Furthermore, the utilization of [Au(CN)₂]⁻, [Pt(CN)₄]²⁻, and [Fe(CN)₆]^{4-/3-} cyanometallates leads to the higher nuclearity aggregates [{Re(diimine)-(CO)₃NC_xM]^{m+} (M = Au, x = 2, **5** and **6**; Pt, x = 4, **7** and **8**; Fe, x = 6, **9** and **10**). All novel compounds were characterized crystallographically. Assemblies **1–8** are phosphorescent both in solution and in the solid state; according to the DFT analysis, the optical properties are mainly associated with charge transfer from Re tricarbonyl motif to the diimine fragment. The energy of this process can be substantially modified by the properties of the ancillary ligands that allows to attain near-IR emission for **3** (λ_{em} = 737 nm in CH₂Cl₂). The Re–Fe^{II/III} complexes **9** and **10** are not luminescent but exhibit low energy absorptions, reaching 846 nm (**10**) due to Re^I → Fe^{III} transition.



INTRODUCTION

Anionic cyanometallates [M(CN)_x]ⁿ⁻/[ML_z(CN)_y]^{m-} occupy a prominent position in the field of coordination-driven supramolecular construction. Chemical stability and high directionality of coordination bonding along with general availability determines their wide utilization as metalloligands in the design of a variety of multinuclear cyano-bridged arrays, which span from the bimetallic complexes to ordered three-dimensional frameworks.^{1–4} Depending on the electronic properties of the constituting metal ions, the resulting compounds exhibit an impressive diversity of physical and chemical behavior. Thus, the inclusion of paramagnetic centers (Cr^{III}, Fe^{III}, Ru^{III}, Co^{II}, etc.) is an established approach to the magnetic polymeric and molecular materials.^{2–4} Combining the metals in different oxidation states (reduced and oxidized), which are capable to communicate electronically via the cyanide linker, leads to the family of mixed-valence species

with appealing optical and redox characteristics, resulting from donor–acceptor (intervalence) charge transfer.^{5–10} In contrast, cyanometallate coordination polymers, particularly those built of relatively flexible [M(CN)₂]⁻ (M = Au, Ag), [AuX₂(CN)₂]⁻ or [PtX₂(CN)₄]²⁻ motifs, which simultaneously comprise weak noncovalent bonding, can exhibit unconventional thermo- and piezo-mechanical features.^{11–15}

Furthermore, dicyanometallates [M(CN)₂]⁻ of coinage metal ions (M = Au, Ag, Cu) and tetracyanoplatinate [Pt(CN)₄]²⁻ have been actively employed for the development of birefringent^{16,17} and photoluminescent^{18–28} homo- and heterobimetallic materials, including sensory systems with distinct optical response to some volatile donor molecules.^{29–32}

Received: October 19, 2018

A notable though less explored route to the cyanometallate-based photofunctional complexes relies on the incorporation of chromophore fragments as constituting elements into the target assemblies. For example, coupling the cyclometalated anions $[\text{IrL}_z(\text{CN})_y]^{m-10,33}$ with Re^{I} (diimine) or Ru^{II} (polypyridine) moieties induces efficient intermolecular $\text{Ir} \rightarrow \text{Re}/\text{Ru}$ energy transfer in the excited state. A similar scenario of $\text{Re} \rightarrow \text{Ru}$ excitation transfer has been described for Re^{I} (diimine)– Ru^{II} (diimine)₂ CN-bridged dyads.⁵ On the contrary, linking the Ru^{II} (polypyridine) centers with Ln^{III} or Cr^{III} units having energetically lower lying excited states sensitizes the M^{III} -centered emission.^{34,35}

Taking into account that the decoration of $[\text{M}(\text{CN})_x]^{n-}$ anions with luminogen components to generate discrete molecular aggregates has been poorly investigated and is mostly focused on the d–f coordination polymers, we intended to prepare a series of heterometallic multichromophore molecules using homoleptic cyanometallates of Au, Pt and Fe as assembling metallogligands. To address this goal, we have chosen $[\text{Re}(\text{diimine})(\text{CO})_3]^+$ (diimine = phenanthroline, bipyridine) photoactive centers as terminal building blocks for supramolecular construction due to their superior and well-studied photophysical properties together with quite facile coordination chemistry.^{36–38}

EXPERIMENTAL SECTION

General Comments. All manipulations were carried out under aerobic conditions, except the synthesis of complex **9**. Starting materials from commercial sources were used as received. $[\text{Re}(\text{phen})(\text{CO})_3(\text{H}_2\text{O})](\text{CF}_3\text{SO}_3)$ and $[\text{Re}(\text{bpy})(\text{CO})_3(\text{H}_2\text{O})](\text{CF}_3\text{SO}_3)$ were prepared in a manner similar to that used for the related complexes^{39,40} by treating $[\text{Re}(\text{diimine})(\text{CO})_3\text{Cl}]$ with AgCF_3SO_3 in acetone.⁴¹ The resultant crude materials were recrystallized by a gas-phase diffusion of diethyl ether into the solutions of titled compounds in wet acetone to afford bright yellow crystalline materials.⁴² $[\text{Re}(\text{phen})(\text{CO})_3(\text{PPh}_3)](\text{CF}_3\text{SO}_3)$ ⁴³ was obtained by treating $[\text{Re}(\text{phen})(\text{CO})_3(\text{H}_2\text{O})](\text{CF}_3\text{SO}_3)$ with PPh_3 in refluxing toluene under a nitrogen atmosphere. $[\text{Au}(\text{PPh}_3)(\text{CN})]^{44}$ was synthesized according to the reported procedures. The solution ¹H and ³¹P{¹H} NMR spectra were recorded on a Bruker 400 MHz Avance spectrometer. Mass spectra were determined on a LC/MS hybrid ultrahigh resolution electrospray quadrupole time-of-flight (UHR ESI-q-TOF) mass spectrometer Bruker MaXis 4G in the ESI⁺ mode. Infrared (IR) spectra were measured on a Bruker Vertex 70 spectrometer. Microanalyses were carried out at the analytical laboratory of the University of Eastern Finland.

$[\text{Re}(\text{bpy})(\text{CO})_3]_2\text{CN}(\text{CF}_3\text{SO}_3)$ (1).⁵ Prepared by a modified procedure. $[\text{Re}(\text{bpy})(\text{CO})_3(\text{H}_2\text{O})](\text{CF}_3\text{SO}_3)$ (50 mg, 0.084 mmol) was dissolved in acetone (4 mL) and treated with a solution of $\text{K}[\text{Ag}(\text{CN})_2]$ (8.3 mg, 0.042 mmol) in methanol (1 mL), causing an immediate precipitation of AgCN . The suspension was stirred overnight in the absence of light. Then, the solids were removed by filtration. Evaporation of the solvent produced a bright yellow-greenish residue, which was recrystallized by a gas-phase diffusion of diethyl ether into its acetone solution at 298 K to give yellow-greenish crystalline material (32 mg, 74%). IR (CH_2Cl_2 , $\nu(\text{CO})$, cm^{-1}): 2037s, 2027s, 1931s. IR (KBr, $\nu(\text{CN})$, cm^{-1}): 2151m. ¹H NMR (acetone-*d*₆, 298 K; δ): 8.91 (dd, $J_{\text{HH}} = 5.4$ and 1.4 Hz, 2H, 2,9-H bpy), 8.85 (dd, $J_{\text{HH}} = 5.4$ and 1.4 Hz, 2H, 2,9-H bpy'), 8.69 (d, $J_{\text{HH}} = 8.1$ Hz, 2H, 5,6-H bpy), 8.63 (d, $J_{\text{HH}} = 8.1$ Hz, 2H, 5,6-H bpy'), 8.42 (m, 4H, 4,7-H bpy and 4,7-H bpy'), 7.75 (m, 4H, 3,8-H bpy and 3,8-H bpy'). ESI⁺ MS (m/z): $[\text{M}]^+$ 878.02 (calcd 878.02). Anal. Calcd for $\text{C}_{28}\text{H}_{16}\text{F}_3\text{N}_5\text{O}_9\text{Re}_2\text{S}$: C, 32.72; H, 1.57; N, 6.81; S, 3.20. Found: C, 32.85; H, 1.73; N, 6.94; S, 3.27.

$[\text{Re}(\text{phen})(\text{CO})_3]_2\text{CN}(\text{CF}_3\text{SO}_3)$ (2). Prepared in a manner analogous to that for **1** from $[\text{Re}(\text{phen})(\text{CO})_3(\text{H}_2\text{O})](\text{CF}_3\text{SO}_3)$ (50 mg, 0.081 mmol) and $\text{K}[\text{Ag}(\text{CN})_2]$ (8.2 mg, 0.041 mmol);

yellow-greenish crystals (29 mg, 67%). IR (CH_2Cl_2 , $\nu(\text{CO})$, cm^{-1}): 2037s, 2028s, 1931s. IR (KBr, $\nu(\text{CN})$, cm^{-1}): 2151m. ¹H NMR (acetone-*d*₆, 298 K; δ): 9.15 (dd, $J_{\text{HH}} = 5.1$ and 1.3 Hz, 2H, 2,9-H phen), 9.07 (dd, $J_{\text{HH}} = 5.1$ and 1.3 Hz, 2H, 2,9-H phen'), 8.95 (dd, 2H, $J_{\text{HH}} = 8.3$ and 1.3 Hz, 4,7-H phen), 8.90 (dd, $J_{\text{HH}} = 8.3$ and 1.3 Hz, 2H, 4,7-H phen'), 8.38 (s, 2H, 5,6-H phen), 8.30 (s, 2H, 5,6-H phen'), 7.97 (m, 4H, 3,8-H phen and 3,8-H phen'). ESI⁺ MS (m/z): $[\text{M}]^+$ 926.02 (calcd 926.02). Anal. Calcd for $\text{C}_{32}\text{H}_{16}\text{F}_3\text{N}_5\text{O}_9\text{Re}_2\text{S}$: C, 35.72; H, 1.50; N, 6.51; S, 2.98. Found: C, 35.93; H, 1.69; N, 6.58; S, 3.05.

$[\text{Re}(\text{phen})(\text{CO})_2(\text{PPh}_3)]_2\text{CN}(\text{CF}_3\text{SO}_3)$ (3). Preparation of $[\text{Re}(\text{phen})(\text{CO})_2(\text{PPh}_3)(\text{NCMe})](\text{CF}_3\text{SO}_3)$. An acetonitrile solution (4 mL) of $[\text{Re}(\text{phen})(\text{CO})_3(\text{PPh}_3)](\text{CF}_3\text{SO}_3)$ (100 mg, 0.116 mmol) was irradiated using a 351 nm pulsed laser (50 mW) for 2.5 h. Then, the solvent was evaporated, and the orange solid was recrystallized by a gas phase diffusion of diethyl ether into its acetone/methanol solution at room temperature to give red crystalline material (71 mg, 70%). IR (CH_2Cl_2 , $\nu(\text{CO})$, cm^{-1}): 1956s, 1889s. ¹H NMR (acetone-*d*₆, 298 K; δ): 9.10 (d, $J_{\text{HH}} = 5.1$ Hz, 2H, 2,9-H phen), 8.82 (dd, 2H, $J_{\text{HH}} = 8.3$ and 1.2 Hz, 4,7-H phen), 8.29 (s, 2H, 5,6-H phen), 7.86 (dd, $J_{\text{HH}} = 8.2$ and 5.1 Hz, 2H, 3,8-H phen), 7.33–7.30 (m, 3H, para-H Ph), 7.26–7.21 (m, 6H, meta-H Ph), 7.17–7.12 (m, 6H, ortho-H Ph). ³¹P{¹H} NMR (acetone-*d*₆, 298 K; δ): 7.2 (s, 1P, PPh_3).

Preparation of $[\text{Re}(\text{phen})(\text{CO})_2(\text{PPh}_3)]_2\text{CN}(\text{CF}_3\text{SO}_3)$. $[\text{Re}(\text{phen})(\text{CO})_2(\text{PPh}_3)(\text{NCMe})](\text{CF}_3\text{SO}_3)$ (50 mg, 0.057 mmol) was dissolved in acetone (5 mL) and treated with a solution of $\text{K}[\text{Ag}(\text{CN})_2]$ (6 mg, 0.029 mmol) in methanol (1 mL), causing an immediate precipitation of AgCN . The suspension was stirred overnight at room temperature in the absence of light. Then, the solids were removed by filtration. Evaporation of the solvents produced a bright red solid, which was recrystallized by a gas-phase diffusion of diethyl ether into its acetone solution at 298 K to give red crystalline material (29 mg, 65%). IR (CH_2Cl_2 , $\nu(\text{CO})$, cm^{-1}): 1933s, 1865s. IR (KBr, $\nu(\text{CN})$, cm^{-1}): 2120m. ¹H NMR (acetone-*d*₆, 298 K; δ): 8.54–8.48 (m, 6H, 2,9-H phen, 2,9-H phen' and 4,7-H phen), 8.44 (d, $J_{\text{HH}} = 8.2$ Hz, 2H, 4,7-H phen'), 8.09 (m, 2H, 5,6-H phen), 8.00 (m, 2H, 5,6-H phen'), 7.47 (dd, $J_{\text{HH}} = 8.2$ and 5.1 Hz, 2H, 3,8-H phen), 7.43 (dd, $J_{\text{HH}} = 8.2$ and 5.1 Hz, 2H, 3,8-H phen'), 7.21–7.16 (m, 6H, para-H Ph and para-H Ph'), 7.10–7.06 (m, 12H, meta-H Ph and meta-H Ph'), 6.98–6.93 (m, 6H, ortho-H Ph), 6.91–6.87 (m, 6H, ortho-H Ph'). ³¹P{¹H} NMR (acetone-*d*₆, 298 K; δ): 31.3 (s, 1P, PPh_3), 26.6 (s, 1P, PPh_3). ESI⁺ MS (m/z): $[\text{M}]^+$ 1396.21 (calcd 1396.21). Anal. Calcd for $\text{C}_{66}\text{H}_{46}\text{F}_3\text{N}_5\text{O}_9\text{P}_2\text{Re}_2\text{S}$: C, 51.32; H, 3.00; N, 4.53; S, 2.08. Found: C, 51.22; H, 3.27; N, 4.57; S, 2.15.

$[\text{Re}(\text{phen})(\text{CO})_3]\text{NCAu}(\text{PPh}_3)](\text{CF}_3\text{SO}_3)$ (4). A solution of $[\text{Au}(\text{PPh}_3)(\text{CN})]$ (50 mg, 0.103 mmol) in dichloromethane (4 mL) was added to a suspension of $[\text{Re}(\text{phen})(\text{CO})_3(\text{H}_2\text{O})](\text{CF}_3\text{SO}_3)$ (64 mg, 0.103 mmol) in dichloromethane (4 mL). The reaction mixture was stirred at room temperature overnight in the absence of light. Then, some precipitate was removed by filtration. Evaporation of the solvent produced a yellow solid, which was recrystallized by a gas-phase diffusion of diethyl ether into its ethanol/dichloromethane solution at 298 K to give green-yellow crystals (64 mg, 59%). IR (KBr, ν , cm^{-1}): (CN) 2183m; (CO) 2033s, 1935s. ESI⁺ MS (m/z): $[\text{M}]^+$ 936.07 (calcd 936.07), $[\text{Au}(\text{PPh}_3)_2]^+$ 721.15, $[(\text{Re}(\text{CO})_3(\text{phen}))_2(\text{NC})_2\text{Au}]^+$ 1148.99. Anal. Calcd for $\text{C}_{35}\text{H}_{23}\text{AuF}_3\text{N}_5\text{O}_6\text{PReS}$: C, 38.75; H, 2.14; N, 3.87; S, 2.96. Found: C, 38.41; H, 2.36; N, 4.07; S, 2.89.

$[\text{Re}(\text{bpy})(\text{CO})_3]\text{NC}_2\text{Au}(\text{CF}_3\text{SO}_3)$ (5). $[\text{Re}(\text{bpy})(\text{CO})_3(\text{H}_2\text{O})](\text{CF}_3\text{SO}_3)$ (50 mg, 0.084 mmol) and $\text{K}[\text{Au}(\text{CN})_2]$ (12 mg, 0.040 mmol) were dissolved in a mixture of acetone (5 mL) and methanol (1 mL), and the reaction mixture was stirred overnight at room temperature in the absence of light. Evaporation of the solvents produced a yellow solid, which was recrystallized by a gas-phase diffusion of diethyl ether into its acetone/methanol solution at 298 K to give light yellow crystalline material (42 mg, 81%). IR (CH_2Cl_2 , $\nu(\text{CO})$, cm^{-1}): 2035s, 1933s. IR (KBr, $\nu(\text{CN})$, cm^{-1}): 2183m. ¹H NMR (acetone-*d*₆, 298 K; δ): 9.16 (dd, $J_{\text{HH}} = 5.4$ and 1.4 Hz, 4H, 2,9-H bpy), 8.81 (d, $J_{\text{HH}} = 8.1$ Hz, 4H, 5,6-H bpy), 8.46 (td, $J_{\text{HH}} = 8.1$ and 1.4 Hz, 4H, 4,7-H bpy), 7.90 (ddd, $J_{\text{HH}} = 8.1$, 5.4, and 1.3 Hz,

4H, 3,8-H bpy). ESI⁺ MS (*m/z*): [M]⁺ 1100.99 (calcd 1100.99). Anal. Calcd for C₂₉H₁₆AuF₃N₆O₉Re₂S: C, 27.84; H, 1.29; N, 6.72; S, 2.56. Found: C, 28.01; H, 1.42; N, 6.80; S, 2.61.

[[Re(phen)(CO)₃NC₂Au](CF₃SO₃)₂ (6). Prepared in a manner analogous to that for **5** from [Re(phen)(CO)₃(H₂O)](CF₃SO₃) (50 mg, 0.081 mmol) and K[Au(CN)₂] (12 mg, 0.041 mmol); yellow crystalline material (38 mg, 72%). IR (CH₂Cl₂, ν (CO), cm⁻¹): 2036s, 1934s. IR (KBr, ν (CN), cm⁻¹): 2187m. ¹H NMR (acetone-*d*₆, 298 K; δ): 9.54 (dd, *J*_{HH} = 5.1 and 1.3 Hz, 4H, 2,9-H phen), 9.05 (dd, *J*_{HH} = 8.3 and 1.3 Hz, 4H, 4,7-H phen), 8.38 (s, 4H, 5,6-H phen), 8.22 (dd, *J*_{HH} = 8.3 and 5.1 Hz, 4H, 3,8-H phen). ESI⁺ MS (*m/z*): [M]⁺ 1148.99 (calcd 1148.99). Anal. Calcd for C₃₃H₁₆AuF₃N₆O₉Re₂S: C, 30.51; H, 1.24; N, 6.47; S, 2.47. Found: C, 30.69; H, 1.50; N, 6.56; S, 2.56.

[[Re(bpy)(CO)₃NC₂Pt](CF₃SO₃)₂ (7). Prepared in a manner analogous to that for **5** from [Re(bpy)(CO)₃(H₂O)](CF₃SO₃) (50 mg, 0.084 mmol) and K₂[Pt(CN)₄] (8 mg, 0.021 mmol); yellow crystalline material (39 mg, 81%). IR (CH₂Cl₂, ν (CO), cm⁻¹): 2034s, 1932s. IR (KBr, ν (CN), cm⁻¹): 2176m. ¹H NMR (acetone-*d*₆, 298 K; δ): 9.06 (dd, *J*_{HH} = 5.4 and 1.4 Hz, 8H, 2,9-H bpy), 8.81 (d, *J*_{HH} = 8.1 Hz, 8H, 5,6-H bpy), 8.52 (td, *J*_{HH} = 8.1 and 1.4 Hz, 8H, 4,7-H bpy), 8.02 (ddd, *J*_{HH} = 8.1, 5.4, and 1.3 Hz, 8H, 3,8-H bpy). ESI⁺ MS (*m/z*): [M]²⁺ 1002.00 (calcd 1002.00), [[Re(CO)₃(bpy)]₃(NC)₃Pt(CN)]⁺ 1579.00. Anal. Calcd for C₅₈H₃₂F₆N₁₂O₁₈PtRe₃S₂: C, 30.25; H, 1.40; N, 7.30; S, 2.78. Found: C, 30.37; H, 1.52; N, 7.43; S, 2.95.

[[Re(phen)(CO)₃NC₂Pt](CF₃SO₃)₂ (8). Prepared in a manner analogous to that for **5** from [Re(phen)(CO)₃(H₂O)](CF₃SO₃) (50 mg, 0.081 mmol) and K₂[Pt(CN)₄] (7.7 mg, 0.020 mmol); bright yellow crystalline material (38 mg, 79%). IR (CH₂Cl₂, ν (CO), cm⁻¹): 2034s, 1932s. IR (KBr, ν (CN), cm⁻¹): 2178m. ¹H NMR (acetone-*d*₆, 298 K; δ): 9.39 (dd, *J*_{HH} = 5.1 and 1.3 Hz, 8H, 2,9-H phen), 9.12 (dd, *J*_{HH} = 8.3 and 1.3 Hz, 8H, 4,7-H phen), 8.42 (s, 8H, 5,6-H phen), 8.34 (dd, *J*_{HH} = 8.3 and 5.1 Hz, 8H, 3,8-H phen). ESI⁺ MS (*m/z*): [M]²⁺ 1050.00 (calcd 1050.00), [[Re(CO)₃(phen)]₃(NC)₃Pt(CN)]⁺ 1651.00. Anal. Calcd for C₆₆H₃₂F₆N₁₂O₁₈PtRe₃S₂: C, 33.04; H, 1.34; N, 7.00; S, 2.67. Found: C, 33.27; H, 1.55; N, 7.11; S, 2.72.

[[Re(bpy)(CO)₃NC₂Fe](CF₃SO₃)₂ (9). [Re(bpy)(CO)₃(H₂O)](CF₃SO₃) (50 mg, 0.084 mmol) was dissolved in acetone (7 mL), and a suspension of K₃[Fe(CN)₆] (5 mg, 0.014 mmol) in methanol (3 mL) was added. The mixture was stirred at room temperature for 12 h in the absence of light under nitrogen atmosphere to give a light-brown solution. Evaporation of the solvents produced a brown oil, which was recrystallized by a gas-phase diffusion of diethyl ether into its acetone/methanol solution at 298 K to give brick-red crystalline material (22 mg, 51%). IR (CH₂Cl₂, ν (CO), cm⁻¹): 2021s, 1906s. IR (KBr, ν (CN), cm⁻¹): 2089m. ¹H NMR (acetone-*d*₆, 298 K; δ): 8.84 (m, *J*_{HH} = 5.4 Hz, 12H, 2,9-H bpy), 8.63 (m, *J*_{HH} = 8.1 Hz, 12H, 5,6-H bpy), 8.41 (m, 12H, 4,7-H bpy), 7.87 (m, 12H, 3,8-H bpy). ESI⁺ MS (*m/z*): [M]²⁺ 1385.00 (calcd 1385.00). Anal. Calcd for C₈₆H₄₈F₆FeN₁₈O₂₄Re₆S₂: C, 33.66; H, 1.58; N, 8.22; S, 2.10. Found: C, 33.73; H, 1.62; N, 8.28; S, 2.14.

[[Re(bpy)(CO)₃NC₂Fe](CF₃SO₃)₃ (10). Prepared in a manner analogous to that for **5** from [Re(bpy)(CO)₃(H₂O)](CF₃SO₃) (50 mg, 0.084 mmol) and K₃[Fe(CN)₆] (5 mg, 0.014 mmol); dark green crystalline material (28 mg, 62%). IR (CH₂Cl₂, ν (CO), cm⁻¹): 2028s, 1914s. IR (KBr, ν (CN), cm⁻¹): 2154m. ¹H NMR (acetone-*d*₆, 298 K; δ): 8.66 (d, *J*_{HH} = 5.4 Hz, 12H, 2,9-H bpy), 8.40 (m, 2H, *J*_{HH} = 8.1 Hz, 12H, 5,6-H bpy), 8.15 (m, 12H, 4,7-H bpy), 7.77 (m, 12H, 3,8-H bpy). Anal. Calcd for C₈₈H₄₈F₉FeN₁₈O₂₇Re₆S₃: C, 32.48; H, 1.50; N, 7.84; S, 2.99. Found: C, 32.71; H, 1.76; N, 7.87; S, 2.97.

X-ray Structure Determinations. The crystals of **2–10** were immersed in cryo-oil, mounted in a Nylon loop, and measured at a temperature of 150 K. The X-ray diffraction data were collected with Bruker Kappa Apex II, Bruker Smart Apex II, and Bruker Kappa Apex II Duo diffractometers using Mo K α radiation (λ = 0.71073 Å). The APEX2⁴⁵ program package was used for cell refinements and data reductions. The structures were solved by direct methods using the SHELXS-2014⁴⁶ program with the WinGX⁴⁷ graphical user interface. A numerical absorption correction (SADABS)⁴⁸ was applied to all data. Structural refinements were carried out using SHELXL-2014.⁴⁶

The crystallization solvent in **2–4** and **6–10** was partially lost from the crystal and could not be resolved unambiguously. The contribution of the missing solvent to the calculated structure factors was taken into account by using a SQUEEZE routine of PLATON.⁴⁹ The missing solvent was not taken into account in the unit cell content.

All hydrogen atoms in **2–10** were positioned geometrically and constrained to ride on their parent atoms, with C–H = 0.95–0.99 Å and *U*_{iso} = 1.2–1.5*U*_{eq} (parent atom). The crystallographic details are summarized in Table S1. Selected structural parameters are listed in Tables S2 and S3.

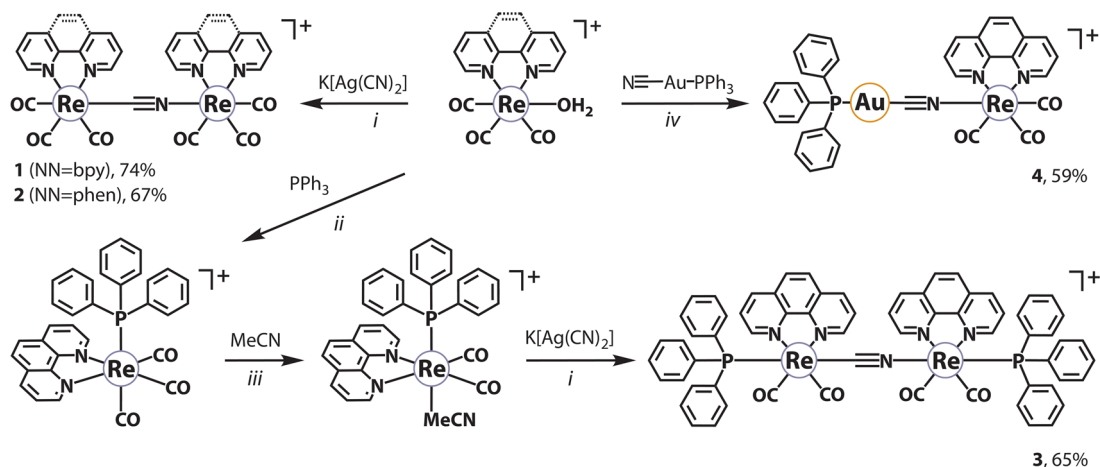
Photophysical Measurements. The photophysical measurements were performed in dichloromethane and methanol solutions, which were carefully deaerated by three “freeze–pump–thaw” cycles. UV/vis absorption spectra were measured on a Shimadzu UV-1800 spectrophotometer; excitation and emission spectra in solution and in the solid state were recorded with a HORIBA FluoroMax-4 spectrofluorometer. Lifetime and emission quantum yields in the solid phase were performed on a HORIBA Scientific FluoroLog-3 spectrofluorometer. The uncertainty of the quantum yield measurement was in the range of $\pm 5\%$ (an average of three replications, which correspond to different orientations of the sample). The emission quantum yield in solutions was determined by the comparative method using coumarin 102 in ethanol (Φ_f = 0.764)⁵⁰ with refraction indexes of dichloromethane and ethanol equal to 1.42 and 1.36, respectively.

Electrochemical Studies. Electrochemical experiments were performed at 298 \pm 1 K in a CH cell using a CH I660 potentiostat (Cambria Scientific, Llynwendy, Llanelli UK). A BAS MF2012 glassy carbon working electrode (GCE) (geometrical area 0.071 cm²), a platinum mesh auxiliary electrode and a platinum wire pseudoreference electrode were used in a conventional three-electrode arrangement. Potentials are provided relative to the Fc/Fc⁺ couple, adding ferrocene (Aldrich) as an internal standard during electrochemical runs. The electrochemistry of complexes **9** and **10** in acetone solutions (HPLC-grade, Carlo Erba reagents) containing 0.10 M Bu₄NPF₆ (Fluka) as a supporting electrolyte was studied after degassing by bubbling Ar for 10 min.

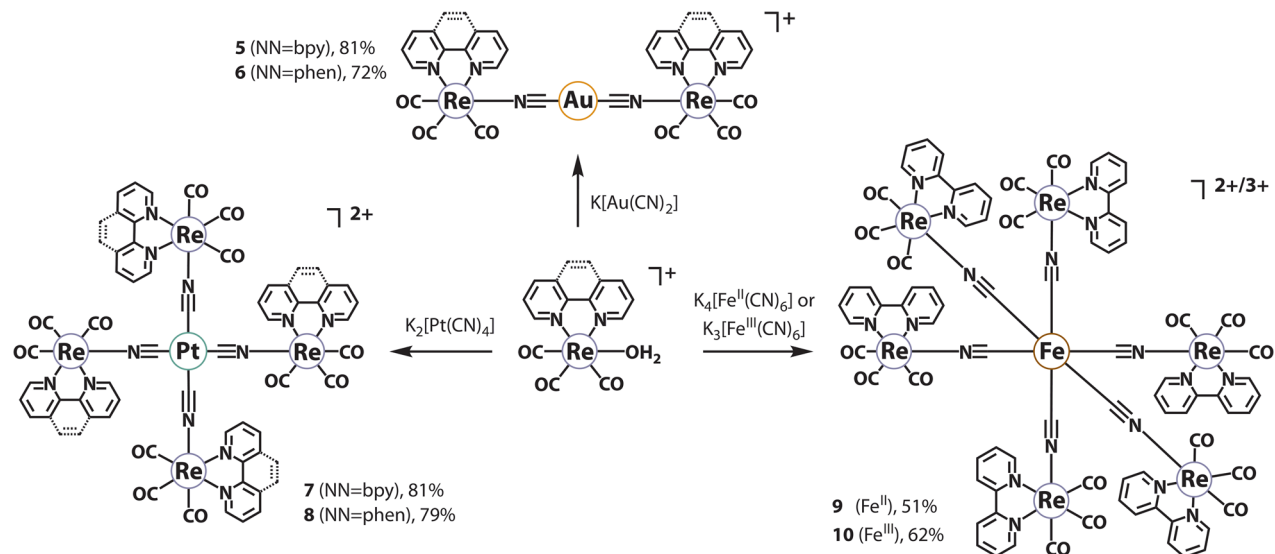
Solid-state experiments were performed at microparticulate films of **9** and **10** prepared by evaporation at air of a drop of an ethanolic solution of the corresponding complex (1 mg/mL) deposited onto the surface of a freshly polished GCE. 0.50 M NaCl aqueous solution was used as a supporting electrolyte.

Computational Details. Compounds **1–10** were studied using the hybrid PBE0 density functional method (DFT-PBE0).^{51,52} All atoms were described by a triple- ζ -valence quality basis set with polarization functions (def-TZVP).⁵³ Multipole-accelerated resolution-of-the-identity technique was used to speed up the calculations.^{54,55} Point group symmetry was used to speed up the calculations (**1–4**: C_s; **5**, **6**: C_{2h}; **7**, **8**: C_{4h}; **9**, **10**: S₆). The used symmetries are lower than the ideal symmetries observed in the NMR experiments because the calculations at 0 K lack the rotational degrees of freedom present at solution state. The geometries of all complexes were first fully optimized within the applied point group using the DFT-PBE0 method. The optimized geometries of the compounds are in good agreement with the available X-ray structures (comparisons of the structural parameters and the XYZ coordinates of the optimized structures are included as Supporting Information, Table S4). The excited states were investigated using the time-dependent DFT formalism.^{56,57} The singlet excitations were determined at the optimized ground-state S₀ geometries, while the lowest energy triplet emissions were determined at the optimized T₁ geometry. In the case of **4** and **7–10**, the TD-DFT calculation of the T₁ state could not be converged due to numerical issues. The calculated excitation and emission wavelengths are strongly red-shifted in comparison to the experiment (Table S5), but the observed trends are reproduced well. All electronic structure calculations were carried out with the TURBOMOLE program package (version 7.3).^{58,59}

Magnetic Susceptibility Measurements. Magnetic data for compound **10** were recorded on a Quantum Design MPMS-5XL

Scheme 1. Syntheses of Complexes 1–4^a

^aReaction conditions: (i) acetone/methanol, room temperature, 12 h; (ii) toluene, 130 °C, 16 h, N₂; (iii) 351 nm pulsed laser, 2.5 h; (iv) dichloromethane, room temperature, 12 h; counterion CF₃SO₃⁻.

Scheme 2. Syntheses of Complexes 5–10 (^a)

^aConditions: acetone/methanol, room temperature, 12 h; counterion CF₃SO₃⁻.

SQUID magnetometer. The polycrystalline sample was compacted and immobilized into a cylindrical PTFE capsule. The data were acquired as a function of the field (0.1–5.0 T) and temperature (2–290 K) and were corrected for diamagnetic contributions of the sample holder (PTFE capsule) and the compound **10** ($\chi_{\text{dia}} = -1.61 \times 10^{-3} \text{ cm}^3 \text{ mol}^{-1}$).

RESULTS AND DISCUSSION

Synthesis and Characterization. The rhenium(I) diimine complexes containing cyanide ligands are not excessive and only a few polynuclear compounds built of the cyanometalated units have been described.^{5,6,60} The available reports though confirm the possibility of using the rigid $-\text{C}\equiv\text{N}-$ linker for the construction of multimetallic assemblies containing Re(I) chromophore motifs. The ability of Re(I) ion to bind both carbon and nitrogen atoms of the CN group offers substantial synthetic flexibility and allows combining the $\{\text{Re}(\text{diimine})(\text{CO})_3\}$ motif with a range of metal centers irrespectively of their affinity to coordinating atoms of the cyanide.

The starting complexes $[\text{Re}(\text{diimine})(\text{CO})_3(\text{H}_2\text{O})](\text{CF}_3\text{SO}_3)$ (diimine = 2,2'-bipyridine, bpy; 1,10-phenanthroline, phen) were readily prepared by the abstraction of Cl⁻ from the parent $[\text{Re}(\text{diimine})(\text{CO})_3\text{Cl}]$ compounds⁴⁰ with AgCF₃SO₃ in wet acetone. Subsequent treatment of the triflate derivatives with 0.5 mol equiv of NaCN however results in a mixture of products and gives the expected bridged species $[\{\text{Re}(\text{diimine})(\text{CO})_3\}_2\text{CN}](\text{CF}_3\text{SO}_3)$ (diimine = bpy **1**,⁵ phen **2**) in small yields. Alternatively, reacting K[Ag(CN)₂] instead of sodium cyanide with 2 equiv of $[\text{Re}(\text{diimine})(\text{CO})_3(\text{H}_2\text{O})](\text{CF}_3\text{SO}_3)$ in acetone/methanol solution leads to the formation of **1** and **2** as the dominant products (Scheme 1).

In order to vary the ligand environment of the dirhenium motif in **2**, the $[\text{Re}(\text{phen})(\text{CO})_3(\text{H}_2\text{O})](\text{CF}_3\text{SO}_3)$ precursor was conventionally converted into the phosphine complex $[\text{Re}(\text{phen})(\text{CO})_3\text{PPh}_3](\text{CF}_3\text{SO}_3)$ in toluene at 130 °C. Further photochemical substitution of the carbonyl group for a labile acetonitrile ligand was achieved by employing a 351

nm pulsed laser (50 mW) under ambient conditions. This mild protocol afforded an intermediate dicarbonyl compound $[\text{Re}(\text{phen})(\text{CO})_2(\text{PPh}_3)(\text{NCMe})(\text{CF}_3\text{SO}_3)]^{61}$ in good yield (70%), but in contrast to commonly used high-pressure mercury lamp irradiation^{62–64} does not require an inert atmosphere and extensive cooling of the system. The formation of the cyano-bridged dinuclear rhenium complex $[\{\text{Re}(\text{phen})(\text{CO})_2(\text{PPh}_3)\}_2\text{CN}](\text{CF}_3\text{SO}_3)$ (**3**) was accomplished by means of similar to the synthesis of compound **2**, using $\text{K}[\text{Ag}(\text{CN})_2]$ as a source of the cyanide linker (Scheme 1). The successful synthesis of **1–3**, in which the $[\text{Re}(\text{diimine})(\text{CO})_3(\text{CN})]$ unit may be considered as a neutral metalloligand, prompted us to extend the methodology to the heterometallic species. Indeed, the dinuclear rhenium(I)–gold(I) complex $[\{\text{Re}(\text{phen})(\text{CO})_3\}\text{NCAu}(\text{PPh}_3)](\text{CF}_3\text{SO}_3)$ (**4**) was obtained by coupling the $[\text{Re}(\text{phen})(\text{CO})_3(\text{H}_2\text{O})](\text{CF}_3\text{SO}_3)$ and $[\text{Au}(\text{PPh}_3)(\text{CN})]^{44}$ constituents at room temperature in the absence of light.

Moreover, decorating the anionic cyanometallates with several cationic $\{\text{Re}(\text{diimine})(\text{CO})_3\}^+$ units has proven to be a facile strategy to attain aggregates of higher nuclearity (Scheme 2). Thus, the reaction of $\text{K}[\text{Au}(\text{CN})_2]$ with $[\text{Re}(\text{diimine})(\text{CO})_3(\text{H}_2\text{O})](\text{CF}_3\text{SO}_3)$ in 1:2 molar ratio efficiently generated the trinuclear $[\{\text{Re}(\text{diimine})(\text{CO})_3\}\text{NC}_2\text{Au}](\text{CF}_3\text{SO}_3)$ complexes (diimine = bpy **5**, phen **6**), though no congener compounds were observed in the case of dicyanoargentate anion as described above (Scheme 1). Pentametallate assemblies $[\{\text{Re}(\text{diimine})(\text{CO})_3\}\text{NC}_4\text{Pt}](\text{CF}_3\text{SO}_3)_2$ (diimine = bpy **7**, phen **8**) were constructed from tetracyanoplatinate(II) dianion and 4 equiv of the corresponding rhenium precursors. Finally, the heptanuclear aggregates $[\{\text{Re}(\text{bpy})(\text{CO})_3\}\text{NC}_6\text{Fe}](\text{CF}_3\text{SO}_3)_n$ **9** ($n = 2$) and **10** ($n = 3$) were prepared by adding the $\{\text{Re}(\text{diimine})(\text{CO})_3\}^+$ blocks to ferro- and ferricyanide salts. The phen analogues of **9** and **10** were not observed presumably due to the steric hindrance caused by the bulkier phenanthroline ligand. Further physical data for each complex was provided through NMR and IR spectroscopies, mass spectrometry, by elemental and X-ray analysis, thus corroborating the attainment of the synthesis of the homo- and heterometallic assemblies.

The ESI⁺ mass spectra of the studied complexes reveal the dominating signals corresponding to singly (**2–6**) and doubly (**7–9**) charged molecular ions, whose m/z values and isotopic patterns are in complete agreement with the calculated ones (Figure S1 and S2). In the case of **4**, in addition to the molecular cation (m/z $[\text{4}]^+ = 936.1$) the signals of $[\text{Au}(\text{PPh}_3)_2]^+$ and $[\{\text{Re}(\text{CO})_3(\text{phen})\}_2(\text{NC})_2\text{Au}]^+$, i.e., $[\text{6}]^+$, species are also observed, indicative of a reversible dissociation and rearrangement of **4** in solution also confirmed by the NMR spectroscopy (see below). The triply charged cation **10** was not detected evidently due to the reduction $\text{Fe}^{3+} \rightarrow \text{Fe}^{2+}$ that occurs under the conditions of ESI-MS experiment and has been noted for other iron(III) compounds.⁶⁵

The ¹H NMR spectra of dirhenium compounds **1–3** demonstrate two similar sets of signals, which belong to the nonequivalent $\{\text{Re}(\text{diimine})\}$ fragments (Figure S3). The given patterns can be attributed to the electronic effect of a nonsymmetrical cyanide bridge. In accordance with this observation, two singlet resonances of 1:1 integral intensities are found in the ³¹P NMR spectrum of **3**. On the contrary, **5–10** display ¹H spectroscopic profiles, indicating that in solution these compounds possess only one type of $\{\text{Re}(\text{diimine})(\text{CO})_3\}$ units (Figures S4 and S5) in compliance with idealized

symmetrical structures depicted in Schemes 1 and 2. The NMR data for complex **4** are compatible with ESI-MS result and point to the existence of several species in solution (Figure S6), which comprise compounds **4**, **6**, and $[\text{Au}(\text{PPh}_3)_2]^+$; the latter is also formed in the course of disproportionation described for the parent $[(\text{PPh}_3)\text{AuCN}]$ complex.⁶⁶

The IR spectra of all titled complexes in the CO stretching region are very much alike and correspond to the indistinguishable rhenium carbonyl motifs with rather minor alterations of the vibrational frequencies. Compounds **9** and **10** with $\{\text{Fe}(\text{CN})_6\}^{n-}$ ($n = 3$ and 4) coordinating anion demonstrate visibly lower energies of vibrations conceivably due to a polyanionic character of the central motif that results in enhanced π -back-donation $d_\pi(\text{Re}) \rightarrow \pi^*(\text{CO})$ and is pronounced for the ferricyanide aggregate **9**. In general, the observed profiles are typical for other diimine di- (**3**) and tricarbonyl (**1**, **2**, and **4–10**) rhenium species. In contrast, the CN vibrations are sensitive to the nature of the central metal atom *M* and vary from 2089 cm^{-1} (**9**, $M = \text{Fe}^{2+}$) to 2187 cm^{-1} (**6**, $M = \text{Au}^+$) that is comparable with the values found for other cyanometallate-bridged species.⁶⁷ Expectedly, the CN frequencies for **9** and **10** differ substantially (2089 and 2154 cm^{-1}) because of a higher π -basicity of the Fe^{2+} center.

The results of crystallographic analysis of **2–10** are shown in Figures 1–3 and S7; Tables S2 and S3 contain selected bond

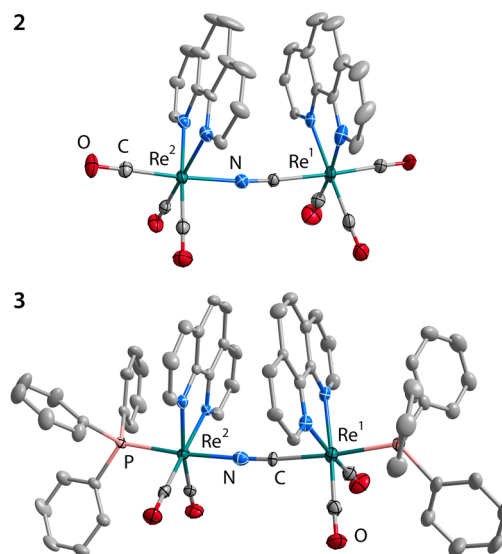


Figure 1. Molecular views of complexes **2** and **3**. Counter ions and hydrogen atoms are omitted for clarity. Thermal ellipsoids are shown at the 50% probability level.

lengths and angles. In all complexes, rhenium ions are hexacoordinated and adopt slightly distorted octahedral environment, formed by the chelating diimine ligand, terminal carbonyl (also phosphine in the case of **3**) and the bridging CN groups. The dirhenium compounds **2** and **3** belong to the same structural type as **1**, which was determined previously⁶⁸ and comprises two $\{\text{Re}(\text{diimine})\}$ fragments linked by an axial cyanide. In both complexes **2** and **3**, the angles $\text{Re}-\text{N}_{\text{CN}}-\text{C}_{\text{CN}}$ and $\text{Re}-\text{C}_{\text{CN}}-\text{N}_{\text{CN}}$ are in the range from 174.4 to 176.9° (Table S2) that gives a nearly linear arrangement of the cyano-bimetallic motif. Analogous to **1**, phenanthroline congener **2** adopts the same eclipsed conformation with torsion angles $\text{N}_{\text{NN}}-\text{Re}-\text{Re}-\text{N}_{\text{NN}}$ of less than 3°. Introducing sterically and electronically different PPh_3 ligands in the axial positions in **3**

causes slight shortening of Re–C_{CN}/N_{CN} distances compared to **2** and results in visible geometry distortions. The latter involves the change of the N_{NN}–Re–Re–N_{NN} torsion to ca. 27° and an increase of the angle between the planes of the phen ligands from 19° (**2**) to 23° (**3**).

Two independent molecules are found in the unit cell of gold–rhenium complex **4**, both having similar structural parameters, which are not exceptional (Table S2). The intermolecular Au...Au separation (3.509 Å) exceeds the sum of van der Waals radii that implies no aurophilic interaction. Though in solution **4** exists as a mixture of several species, its crystallization gives phase pure material, which contains only the bimetallic complex, shown in Figure 2, as confirmed by PXRD analysis (Figure S8).

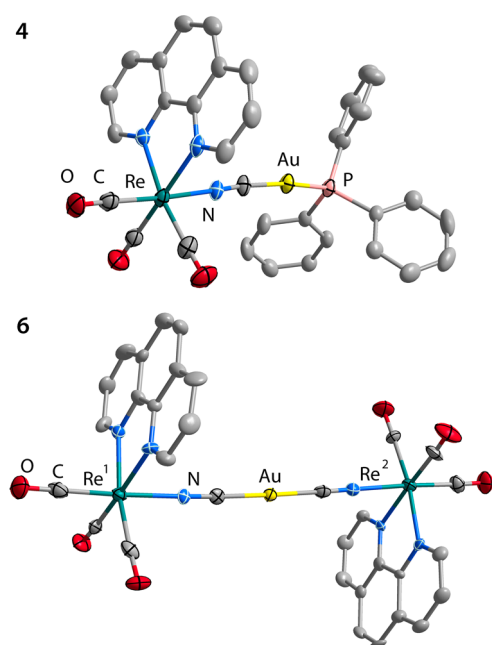


Figure 2. Molecular views of complexes **4** and **6**. Counter ions and hydrogen atoms are omitted for clarity. Thermal ellipsoids are shown at the 50% probability level.

Dicyanoaurate-bridged compounds **5** and **6** demonstrate different molecular packings, which evidently determine their solid-state molecular geometries (Figures 2 and S7). Thus, **5** has an eclipsed configuration, resembling that of **2**, and a substantial deviation of Re–NC–Au–CN–Re chain from linearity ($\angle\text{Re–Au–Re} = 165.4^\circ$). Conversely, phenanthroline complex **6** has a staggered conformation of {Re(phen)} units and Re–Au–Re angle of 175.4°.

Both pentanuclear complexes **7** and **8** feature the expected square-planar cyanoplatinate core, which holds four {Re(diimine)(CO)₃} fragments (Figures 3 and S7). Their mutual orientation is apparently defined by the steric requirements of the diimine ligands, which determine the distortion of structure **7** from the idealized square shape. The packings of complexes **6**–**8** show non-negligible intermolecular π – π stacking interactions between the diimine ligands of adjacent molecules with interplanar distances of 3.60, 3.30, and 3.55 Å, respectively (Figure S9).

The rhenium–iron assemblies **9** and **10** consist of the central six-coordinated Fe^{II} and Fe^{III} ions, respectively, which are surrounded by six rhenium units giving nearly regular

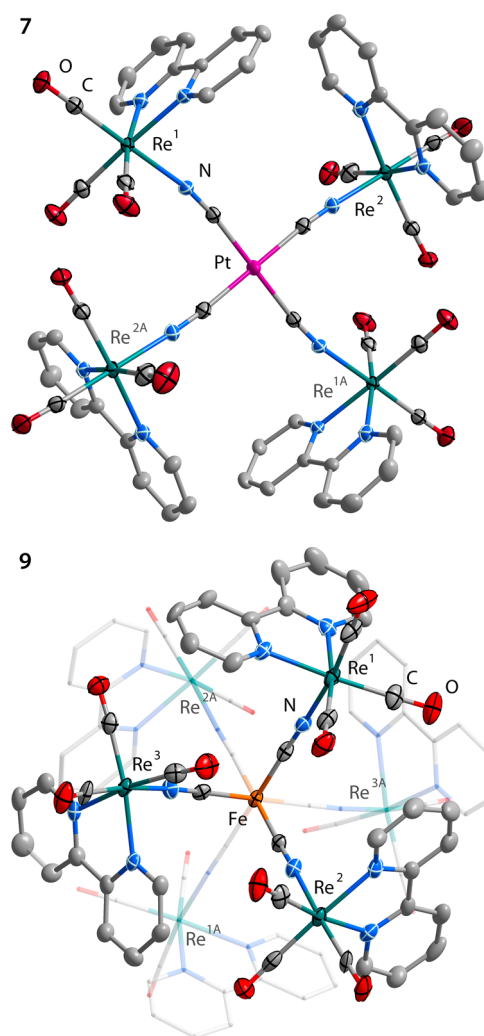


Figure 3. Molecular views of complexes **7** and **9**. Counter ions and hydrogen atoms are omitted for clarity. Thermal ellipsoids are shown at the 50% probability level.

octahedral shape of the resultant heptanuclear species (Figures 3 and S7). The molecular symmetry of **9** and **10** in the crystals is lower than that in solution, where all the pendant {Re(bpy)} groups become indistinguishable. Nevertheless, the deviation of the structural parameters among three crystallographically inequivalent groups of metalloligands [Re(bpy)(CO)₃NC] in each of the complex are quite minor (Table S3) supporting their easy symmetrization in the fluid medium. The change of the oxidation state of the Fe ion (+2 in **9**, +3 in **10**) does not have a significant impact on the molecular arrangement. For example, the Fe–C bond lengths remain virtually unaffected (average distances are 1.924 and 1.929 Å for **9** and **10**), while the Re–N contacts experience slight elongation in **10** (avg 2.135 Å vs 2.122 Å in **9**) that might be attributed to the less favorable electrostatics upon increase of the overall positive charge. The structural data for **9** and **10** in general agree well with those reported for the congener neutral molecule [Re(dmb)(CO)₃]₃[Fe(CN)₆] (dmb = 4,4'-dimethyl-2,2'-bipyridine).⁶ The latter compound and its di/trinuclear congeners represent virtually the only examples of cyanometallate linkers furnished with {Re(diimine)} chromophores. Moreover, complexes [M(CN)_x][M'L_y]_x (M = Pt, x = 4; Fe, x

= 6) with all bridging cyanide ligands represent as a quite limited class of molecular aggregates.^{69–72}

Photophysical Properties. The electronic absorption spectra of complexes **1**, **2**, and **5–8** (Figure 4 and Table 1)

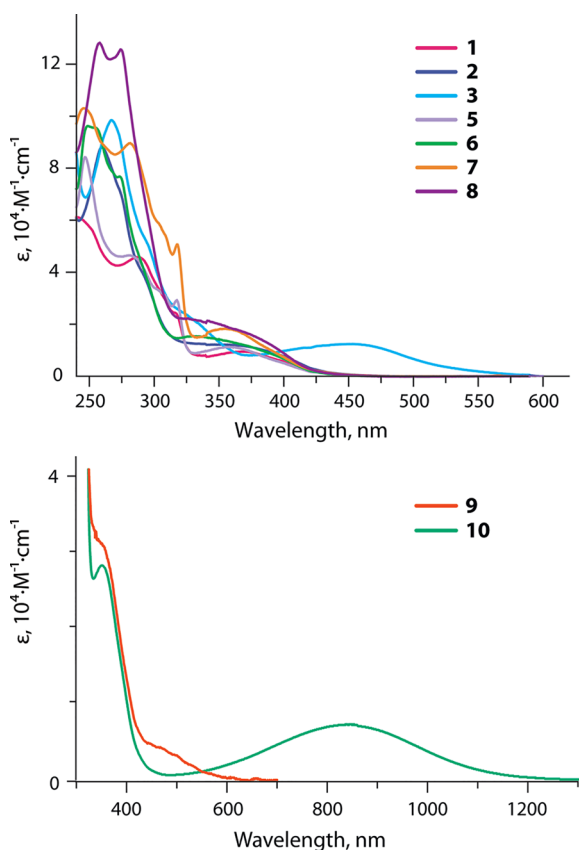


Figure 4. Electronic absorption spectra of complexes **1–3**, **5–8** (CH_2Cl_2) and **9** and **10** (MeOH), 298 K.

are determined by the $\{\text{Re}(\text{diimine})(\text{CO})_3\}$ chromophores and thus are reminiscent to those of a variety of previously studied rhenium(I) compounds,^{5,40,73–75} the optical properties of **4** were investigated only in the solid state due to the aforementioned dissociation in solution. Analogously to the earlier assignments, the intense high-energy absorption bands in the region of 220–320 nm for the title compounds likely correspond to the intraligand $\pi-\pi^*$ transitions. The lower energy bands, which are centered around 350 nm with tails extending up to 450 nm, are ascribed to the charge transfer

from $\{\text{Re}(\text{CO})_3\}$ fragment to the diimine ligand. Computational analysis confirms the proposed nature of the lowest energy excitations $S_0 \rightarrow S_1$ (Figures S10–S12), which also involve cyanide groups in the case of **1** and **3**. High molar absorptivities of the charge transfer bands (350–370 nm, $\epsilon > 10^4 \text{ M}^{-1} \text{ cm}^{-1}$) indicate their certain mixing with IL character and are also consistent with the presence of several chromophores in the same molecular entity.^{76,77} In the case of **3**, the substitution of carbonyl groups in *trans*-position to the cyanide bridge for triphenylphosphine ligands results in a considerable redshift of the longest wavelength absorption band ($\lambda_{\text{abs}} = 456 \text{ nm}$) compared to the tricarbonyl compounds. This behavior is evidently related to a weaker π -accepting ability of PPh_3 with respect to carbonyl group that destabilizes the $d\pi(\text{Re})$ orbitals in **3** and, consequently, lowers the HOMO–LUMO gap.^{62,76,78} Recently, even a more pronounced decrease of the energy gap has been described for $[\text{Re}(\text{deeb})(\text{CO})_2(\text{PMe}_3)\text{Cl}]$ (deeb = 4,4'-diethylester-2,2'-bipyridine) complex.⁷⁹ Interestingly, in **1–3**, the excited state is predicted to engage the Re^1 blocks connected to the N atom of the cyanide spacer (Figure S10).

The Re–Fe compounds display additional features which are associated with iron hexacyanide motif. Thus, a relatively weak band at ca. 480 nm, identified in the spectrum of **9** is not observed for the individual components $[\text{Fe}(\text{CN})_6]^{4-80}$ and $[\text{Re}(\text{bpy})(\text{CO})_3\text{CN}]$.⁵ Therefore, it is likely to originate from electronic transitions localized within the $[\text{Fe}^{\text{II}}(\text{CN})_6]^{4-}$ coordinating anion perturbed by $\{\text{Re}(\text{diimine})(\text{CO})_3\}$ groups and mixed with some $\text{Fe}^{\text{II}} \rightarrow \text{bpy}$ charge transfer (Figure S12).

Complex **10**, which is derived from **9** via one-electron oxidation of the iron center, exhibits a rather intense broad near-infrared band at 846 nm ($\epsilon = 7 \times 10^3 \text{ M}^{-1} \text{ cm}^{-1}$ in methanol, Figure 4) that can be assigned to a MM'CT $\text{Re}^1 \rightarrow \text{Fe}^{\text{III}}$ transition by analogy with $\text{Re}^1\text{–Fe}^{\text{III}6}$ and the related $\text{Ru}^{\text{II}}\text{–Fe}^{\text{III}}$ mixed-valence compounds.^{7,9} In line with the trend observed for $[\text{Re}^1(\text{dmb})(\text{CO})_3]_n[\text{Fe}^{\text{III}}(\text{CN})_6]^{n-3}$ ($n = 1\text{–}3$) congeners, which absorb in methanol at 578, 610, and 649 nm, respectively,⁶ increasing the number of peripheral $\{\text{Re}(\text{bipy})\}$ fragments in aggregate **10** to $n = 6$ substantially decreases the energy of the MM'CT band and simultaneously enhances the molar absorptivity.

Complexes **1–8** display photoluminescence in solution and in the solid state under ambient conditions; the relevant data are provided in Tables 1 and 2. Re–Fe assemblies **9** and **10** are not emissive as their lowest energy excited states are dominated by the $[\text{Fe}(\text{CN})_6]^{4-/3-}$ fragments (see Figure S12), which can accept higher energy excitation from the

Table 1. Photophysical Properties of Complexes **1–3** and **5–10** in Solution

	λ_{abs} nm ($\epsilon \cdot 10^4 \text{ M}^{-1} \text{ cm}^{-1}$)	λ_{em} (nm) ^a	Φ (aer/deg) (%) ^b	τ_{obs} (μs)	k_{r} (s^{-1}) ^c	k_{nr} (s^{-1}) ^d
1 ^e	287 (4.6), 315 (2.4), 368 (1.0)	571 (515)	7/10	0.4	2.5×10^5	2.2×10^6
2	260 (8.8), 287 (4.4), 355 (1.2)	564 (515)	12/30	1.6	1.9×10^5	4.4×10^5
3	267 (9.8), 321 (2.5), 456 (1.2)	737 (606)	–/<1	0.023		
5	246 (8.4), 281 (4.7), 317 (2.9), 359 (1.1)	554 (504)	11/19	0.6	3.2×10^5	1.4×10^6
6	249 (9.6), 254 (9.5), 273 (7.7), 330 (1.6)	543 (505)	15/48	1.9	2.5×10^5	2.7×10^5
7	246 (10.3), 281 (9.0), 305 (5.7), 318 (5.1), 355 (1.8)	560 (519)	10/21	0.5	4.2×10^5	1.6×10^6
8	257 (12.5), 274 (12.5), 338 (2.2)	549 (516)	12/42	2.2	1.9×10^5	2.6×10^5
9	239 (17.6), 281 (14.0), 315 (8.8), 352 (3.1), 480 (0.4)					
10	243 (15.0), 280 (11.9), 316 (8.0), 351 (2.8), 846 (0.7)					

^aValues in parentheses correspond to frozen solutions at 77 K. ^b $\lambda_{\text{ex}} = 365 \text{ nm}$; ^c $k_{\text{r}} = \Phi/\tau_{\text{obs}}$; ^d $k_{\text{nr}} = k_{\text{obs}} - k_{\text{r}} = (1-\Phi)/\tau_{\text{obs}}$. ^e CH_2Cl_2 for **1–3** and **5–8**; methanol for **9** and **10**.

Table 2. Solid-State Photophysical Properties of Complexes 1–8 at 298 K

	λ_{em} (nm)	Φ (%) ^a	τ (μ s)	k_r (s ⁻¹) ^b	k_{nr} (s ⁻¹) ^c
1	523	19	1.0	1.9×10^5	8.1×10^5
2	528	22	2.5	8.8×10^4	3.1×10^5
3	637	2	0.1	2.0×10^5	9.8×10^6
4	534	25	2.4	1.0×10^5	3.1×10^5
5	522	31	1.0	3.1×10^5	6.9×10^5
6	562	3	0.6	5.0×10^5	1.2×10^6
7	547	14	0.5	2.8×10^5	1.7×10^6
8	549	19	1.5	1.3×10^5	5.4×10^5

$$^a \lambda_{ex} = 340 \text{ nm. } ^b k_r = \Phi/\tau_{obs}. \quad ^c k_{nr} = k_{obs} - k_r = (1 - \Phi)/\tau_{obs}.$$

Re(bpy) fragments and then relax nonradiatively. In degassed dichloromethane, complexes **1**, **2**, and **5–8** bearing tricarbonyl rhenium motifs exhibit greenish to yellow photoemission (Figure 5) with quantum yields ranging from 10% (**1**) to 48% (**6**), which are systematically higher for phen-containing compounds. The structureless profiles of the bands, their wavelengths, and long lifetimes ($\tau_{obs} = 0.4\text{--}2.2 \mu\text{s}$) are compatible with the triplet nature of the emissive excited state (³MLCT, where M actually represents the entire Re(CO)₃ unit), which is typical for rhenium tricarbonyl species with bpy and phen ligands.^{40,73,81,82} DFT calculations clearly support the ³MLCT assignment (Figures S10–S12). In comparison to the reported [Re(bpy)(CO)₃CN]^{5,83,84} ($\lambda_{em} = 591 \text{ nm}$ in CH₂Cl₂), the emissions of bpy-containing compounds **1** ($\lambda_{em} = 571 \text{ nm}$), **5** ($\lambda_{em} = 554 \text{ nm}$), and **7** ($\lambda_{em} = 560 \text{ nm}$) are found at visibly shorter wavelengths and demonstrate longer observed lifetimes. This eventually reflects the electronic effect of M–CN → Re coordination in multimetallic species versus terminal NC → Re bonding in the mononuclear predecessor.

In the case of complexes **1** and **2**, which contain two chemically nonequivalent {Re(diimine)(CO)₃} fragments, i.e., C- and N-bound chromophores, we were not able to detect dual emission under steady-state conditions. Using different excitation wavelengths and monitoring the excitation spectra at high and low energy sides of the emission bands produced identical spectroscopic profiles (Figure S13). The lifetime measurements at 500 and 680 nm gave virtually the same values of τ_{obs} for each complex **1** and **2** (within an experimental error) and confirmed the monoexponential decay. This surveillance likely suggests that there is one emissive excited state, which is localized on the N-coordinated rhenium fragment according to the DTF analysis (Figure S10) and

indicates fast energy transfer (diimine)Re → CN → Re–(diimine) in these dirhenium systems.

The replacement of the bpy ligand (in **1**, **5**, and **7**) for phen (**2**, **6**, and **8**) in rhenium fragments conceivably alters the energetics of MLCT and results in some hypsochromic shifts of the emission maxima that has been noted earlier for other [Re(diimine)(CO)₃L] luminophores^{85–87} and qualitatively reproduced computationally (Table S5). Furthermore, the phosphorescence quenching of phenanthroline-based compounds **2**, **6**, and **8** by molecular oxygen is higher than for the bipyridyl-containing chromophores, because in the former case the collisional quenching by O₂ is evidently more effective due to greater spatial accessibility of the phenanthroline aromatic system and longer lifetime of the corresponding excited state. In contrast, the cyanometallate bridges, [Au(CN)₂]⁻ and [Pt(CN)₄]²⁻, have a very small contribution into the frontier molecular orbitals participating in the electronic transitions and therefore show a negligible effect on the photophysical properties of the studied multimetallic assemblies. The DFT excited state density difference plots in Figure S11 clearly illustrate that the orbitals of the Au atoms are not implicated at all into the T₁ → S₀ emission of **5/6**. Despite the calculation of the T₁ state for **7/8** did not converge, the S₀ → S₁ excitations for these Re–Pt species involve only the rhenium fragments (Figure S12), meaning that their lowest lying triplet states likely are also localized on {Re(diimine)(CO)₃} motifs. The similarity of the emission characteristics for **5/6** and **7/8** supports this conclusion.

On the basis of the absorption data analysis, the emission of complex **3**, substituted with triphenylphosphine ligands, is expectedly redshifted in comparison to its predecessor **2** ($\lambda_{em} = 564 \text{ nm}$) and appears in the near-IR (NIR) region ($\lambda_{em} = 737 \text{ nm}$, Figure 5). Such dramatic decrease in emission energy with respect to **2** ($\Delta\nu = 4162 \text{ cm}^{-1}$) arises from introducing the less π -acidic phosphine ligand instead of the carbonyl group that eventually rises the energy of the ground state.⁷⁹ A substantially shorter observed lifetime for **3** ($\tau_{obs} = 23 \text{ ns}$) results from much lower quantum efficiency ($\Phi_{em} < 1\%$) that is a natural consequence of the “energy gap law”.⁸⁸ The cases of fast nonradiative relaxation were described for some other dicarbonyl Re(I) compounds having axial substituents with a weak ligand field.^{62,79} Although **3** shows low quantum yield in solution of less than 1%, it illustrates that NIR phosphorescence, which is still rare among rhenium(I) diimine species,^{82,89–91} can be achieved without demanding modification of the diimine fragment but through adjusting the

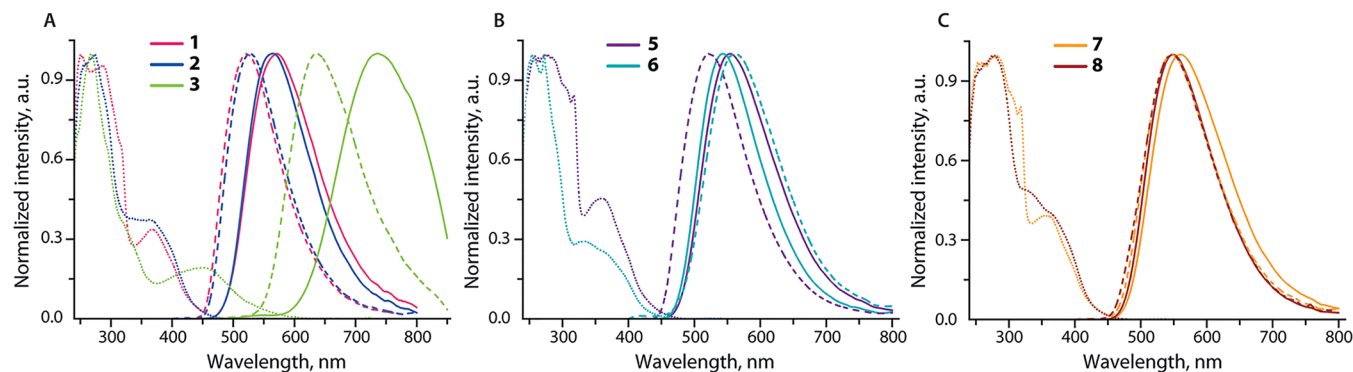


Figure 5. Normalized excitation (dotted lines) and emission spectra of complexes **1–3** and **5–8** in dichloromethane solution (solid lines); dashed lines correspond to solid-state emission at 298 K.

energy of the d orbitals via modification of the electronic properties of the ancillary ligands. The given trend in energies is also reproduced theoretically (Table S5), though the predicted wavelengths for 1–3 are visibly underestimated. These spectroscopic features contrast with luminescence characteristics of diisocyanide-linked congeners $[\{\text{Re}(\text{phen})(\text{CO})_2(\text{PPh}_3)_2(\text{CN}-\text{R}-\text{NC})\}]^{2+}$ ($\lambda_{\text{em}} = 564\text{--}566$ nm, $\Phi_{\text{em}} = 13\text{--}17\%$)⁷⁶ pointing to the crucial role of electron density on the rhenium atoms, modulated by the bridging unit. In frozen solution at 77 K, the emission bands for all compounds 1–3 and 5–8 demonstrate substantial blue shift with respect to the values obtained at 298 K (Table 1 and Figure S14); the energies for tricarbonyl complexes become nearly identical. Such rigidochromic effect is often encountered for rhenium diimine luminophores with ³MLCT excited state, which can get destabilized in a rigid environment.^{92–94}

The difference between the solution and the solid-state emissions at 298 K gradually diminishes with the growth of the number of $\{\text{Re}(\text{diimine})\}$ fragments and becomes virtually negligible for Re–Pt complexes 7 and 8 (Figure 5, Table 2), which probably reflects an increasing intramolecular rigidity due to steric confinements. Otherwise, the emission profiles, lifetimes, and the radiative rate constants obtained for the crystalline samples are very close to those found in solution, meaning that in both phases the emissive excited state has the same origin, i.e., predominantly ³MLCT, and very similar environment properties.

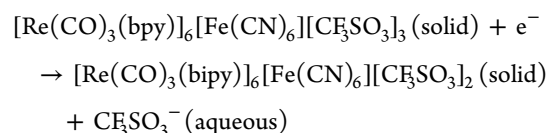
Heterometallic Re–Au complex 4, which was investigated in the crystalline form only, features green luminescence band of moderate intensity ($\Phi_{\text{em}} = 25\%$) maximized at 534 nm (Figure S15). The photophysical parameters for 2 and 4 are nearly the same, including the identity of their excitation spectra 4 (Figure S15). These experimental data are in line with DFT results (Figure S10) and suggest no appreciable contribution of phosphino-gold cyanide motif to the observed emission of 4, which originates exclusively from the $\{\text{Re}(\text{phen})\}$ fragment, similarly to other rhenium(I)–gold(I) phosphine complexes.^{74,95}

Electrochemical and Magnetic Properties of 9 and 10. The electrochemical response of complexes 9 and 10, containing redox active iron centers, has been studied in acetone solution and in the solid state in contact with aqueous electrolytes in order to provide complementary electrochemical information, using the voltammetry of microparticles methodology^{96,97} previously employed for characterizing a series of polymetallic compounds.^{98,99}

The cyclic voltammograms of 9 and 10 in acetone solution (Figure S16) show that in both cases a quasi-reversible one-electron couple (as judged by the cathodic-to-anodic peak potential separation approaching 60 mV at low scan rates) was recorded at potentials near to that of the Fc/Fc^+ couple accompanied by a prominent irreversible oxidation process at ca. +1.0 V. The latter process can be attributed to the oxidation of Re^{I} ions, while the reversible couple is assigned to the oxidation/reduction of the hexacyanoferrate(II/III) groups that correlates with the literature data.^{5,6,79,100} Remarkably, the formal electrode potential (calculated as the half-sum of the cathodic and anodic peak potentials) of complex 9 (−0.050 V vs Fc/Fc^+) differs significantly from that of complex 10 (−0.280 V vs Fc^+/Fc), as shown in Figure S16. No changes in the voltammetric response of 10 were detected upon aeration of its solution, whereas under the exposure to air 9 gives rise to an additional reversible couple centered at +0.230 V vs Fc/Fc^+

that is increased progressively and likely indicates the chemical oxidation of Fe^{II} leading to the degradation of 9. These features can be interpreted on assuming that there are differences between the coordinative arrangement of the hexacyanoferrate-(II/III) centers in complexes 9 and 10 in solution, possibly involving some dissociation of the pendant $\{\text{Re}(\text{bpy})\}$ fragments and solvent interaction¹⁰¹ in the case of complex 9.

The voltammetry of microparticulate films of both complexes are essentially very similar in the solid state after one or two potential cycles. As can be seen in Figure S16, in contact with air-saturated 0.50 M NaCl a one-electron reversible couple is recorded at +0.71 V vs Ag/AgCl in both cases with no apparent interaction with dissolved oxygen, which displays a cathodic wave at −0.60 V. This signal can be interpreted in the light of our previous studies on some Fc-functionalized complexes,^{98,99} on the assumption that assemblies 9 and 10 display solid-state electrochemical reduction/oxidation processes involving the insertion/deinsertion of CF_3SO_3^- ions:



The relevant point to emphasize is that the overall reaction proceeds reversibly and virtually the same way for complexes 9 and 10 thus denoting that there are no substantial coordinative differences between them in the solid state.

The hexacyanoferrate(II/III) compounds are known to contain low-spin $\text{Fe}^{\text{II/III}}$ ions. To confirm that coordination of $\{\text{Re}(\text{bpy})\}$ fragments did not change substantially the ligand field strength and retained the spin state of the central ion, the magnetic data for compound 10 were measured and are presented in Figure S17A as $\chi_{\text{m}}T$ versus T curve at 0.1 T and as M_{m} versus B curve at 2.0 K. The $\chi_{\text{m}}T$ curve reaches a value at 290 K of 0.794 $\text{cm}^3 \text{K mol}^{-1}$, which is typical for low-spin Fe^{III} centers due to the ²T_{2g} ground term that generates distinct contributions from orbital momentum. Thus, $\chi_{\text{m}}T$ is considerably larger than the spin-only contribution of a $S = 1/2$ system (0.375 $\text{cm}^3 \text{K mol}^{-1}$ assuming $g = 2.0$). The purity of complex 10 with respect to ferro- or ferrimagnetic impurities has been checked by measurements at different magnetic fields; the corresponding $\chi_{\text{m}}T$ versus T curve at 0.1–3.0 T is illustrated in Figure S17B. Since we do not observe any notable divergence of the $\chi_{\text{m}}T$ curves at $T > 200$ K, potential impurities can be excluded. By lowering the temperature, $\chi_{\text{m}}T$ continuously decreases to a minimum at 2.0 K and reaches a value of 0.385 $\text{cm}^3 \text{K mol}^{-1}$, which is close to the expected value for a $S = 1/2$ single ion. The magnetization curve at 2.0 K shows a magnetization of $M_{\text{m}} \approx 0.9 N_{\text{A}}\mu_{\text{B}}$ at 5.0 T. Although M_{m} is not saturated, the slope of M_{m} hints at a saturation value of ca. 1 $N_{\text{A}} \mu_{\text{B}}$ indicating a ground state of $S = 1/2$ derived from the equation $M_{\text{m,sat}} = gSN_{\text{A}}\mu_{\text{B}}$.

CONCLUSIONS

We described the supramolecular construction of a series of homo- and heterometallic complexes composed of rhenium(I) diimine tricarbonyl chromophores along with linking cyanide (1–4) and cyanometallate (5–10) anions. The polydentate nature of the central fragments $[\text{M}(\text{CN})_x]^{n-}$ allows to vary the nuclearity of the target assemblies and therefore the decoration of $[\text{Au}(\text{CN})_2]^-$, $[\text{Pt}(\text{CN})_4]^{2-}$, and $[\text{Fe}(\text{CN})_6]^{3-/4-}$ motifs with

{Re(diimine)} blocks affords tri- (5, 6), penta- (7, 8), and heptametallic (9, 10) species, respectively. The spectroscopic investigations of 1–8 reveal that their optical properties are governed by the rhenium(I) constituents with negligible contribution of the heterometals into the lowest lying excited state. The luminescence of complexes 1–8 is associated with electronic transitions predominantly of ³MLCT character; the assignment is supported by theoretical analysis. In solution, the yellow emission of bpy-containing compounds 1, 5, and 7 ($\lambda_{\text{em}} = 554\text{--}571\text{ nm}$) is systematically red-shifted with respect to phen congeners 2, 6, and 8 ($\lambda_{\text{em}} = 543\text{--}564\text{ nm}$), which also demonstrate higher intensity with maximum quantum yield of 48% (Re–Au complex 6) and a more pronounced quenching by molecular oxygen. In contrast, axially PPh₃-substituted dirhenium compound 3 shows NIR phosphorescence ($\lambda_{\text{em}} = 737\text{ nm}$) that is attributed to the destabilizing effect of the phosphine ligand on the d orbitals of the metal. The lack of luminescence in the case of heptanuclear Re–Fe aggregates 9 and 10 is related to the active role of [Fe(CN)₆]^{4-/3-} polyanions in the lowest lying excited state. In particular, the presence of Fe^{III} center induces intermetallic Re^I → Fe^{III} charge transfer that results in the intense NIR absorption ($\lambda_{\text{abs}} = 846\text{ nm}$, $\epsilon = 7 \times 10^3\text{ M}^{-1}\text{ cm}^{-1}$). The electrochemical behavior of these compounds shows essentially irreversible oxidation of the Re^I ions that is accompanied by a quasi-reversible one-electron redox process of the [Fe^{II/III}(CN)₆]^{4-/3-} groups. The magnetic susceptibility measurement of 10 confirms the low-spin configuration of the iron(III), which is retained upon binding to the rhenium(I) fragments. Overall, the titled cyano-bridged aggregates illustrate a simple but efficient synthetic approach to discrete supramolecular coordination complexes with versatile physical properties.

■ ASSOCIATED CONTENT

● Supporting Information

The Supporting Information is available free of charge on the ACS Publications website at DOI: 10.1021/acs.inorgchem.8b02974.

Crystallographic and computational details, molecular views of selected complexes, ESI-MS, NMR and additional photophysical data, electron density difference plots (PDF)

Optimized Cartesian coordinates of complexes 1–9 (XYZ)

Accession Codes

CCDC 1873812–1873820 contain the supplementary crystallographic data for this paper. These data can be obtained free of charge via www.ccdc.cam.ac.uk/data_request/cif, or by emailing data_request@ccdc.cam.ac.uk, or by contacting The Cambridge Crystallographic Data Centre, 12 Union Road, Cambridge CB2 1EZ, UK; fax: +44 1223 336033.

■ AUTHOR INFORMATION

Corresponding Authors

*E-mail: igor.koshevoy@uef.fi (I.O.K.).

*E-mail: antti.karttunen@aalto.fi (A.J.K.).

ORCID

Antonio Doménech-Carbó: 0000-0002-5284-2811

Kirill Yu. Monakhov: 0000-0002-1013-0680

Igor O. Koshevoy: 0000-0003-4380-1302

Notes

The authors declare no competing financial interest.

■ ACKNOWLEDGMENTS

This research has been supported by grant of the Russian Science Foundation (16-13-10064, E.V.G., spectroscopic and photophysical studies) and the Finnish National Agency for Education (CIMO fellowship to K.S.K., synthesis and structural characterization). The work was performed using the equipment of the Analytical Centre for Nano- and Biotechnologies (Peter the Great St Petersburg Polytechnic University with financial support from the Ministry of Education and Science of Russian Federation); Centers for Magnetic Resonance, for Optical and Laser Materials Research, for Chemical Analysis and Materials Research, Research Park of St. Petersburg State University. We thank Dr. Jan van Leusen (Institut für Anorganische Chemie, RWTH Aachen University) for helpful discussions and suggestions.

■ REFERENCES

- (1) Alexandrov, E. V.; Virovets, A. V.; Blatov, V. A.; Peresyphina, E. V. Topological Motifs in Cyanometallates: From Building Units to Three-Periodic Frameworks. *Chem. Rev.* **2015**, *115*, 12286–12319.
- (2) Wang, S.; Ding, X.-H.; Zuo, J.-L.; You, X.-Z.; Huang, W. Tricyanometalate molecular chemistry: A type of versatile building blocks for the construction of cyano-bridged molecular architectures. *Coord. Chem. Rev.* **2011**, *255*, 1713–1732.
- (3) Wang, S.; Ding, X.-H.; Li, Y.-H.; Huang, W. Dicyanometalate chemistry: A type of versatile building block for the construction of cyanide-bridged molecular architectures. *Coord. Chem. Rev.* **2012**, *256*, 439–464.
- (4) Li, Y.-H.; He, W.-R.; Ding, X.-H.; Wang, S.; Cui, L.-F.; Huang, W. Cyanide-bridged assemblies constructed from capped tetracyanometalate building blocks [MA(ligand)(CN)₄]^{1-/2-} (MA = Fe or Cr). *Coord. Chem. Rev.* **2012**, *256*, 2795–2815.
- (5) Kalyanasundaram, K.; Grätzel, M.; Nazeeruddin, M. K. Luminescence and Intramolecular Energy-Transfer Processes in Isomeric Cyano-Bridged Rhenium(I)-Rhenium(I) and Rhenium(I)-Ruthenium(II)-Rhenium(I) Polypyridyl Complexes. *Inorg. Chem.* **1992**, *31*, 5243–5253.
- (6) Pfennig, B. W.; Cohen, J. L.; Sosnowski, I.; Novotny, N. M.; Ho, D. M. Synthesis, Characterization, and Intervalence Charge Transfer Properties of a Series of Rhenium(I)-Iron(III) Mixed-Valence Compounds. *Inorg. Chem.* **1999**, *38*, 606–612.
- (7) Alborés, P.; Rossi, M. B.; Baraldo, L. M.; Slep, L. D. Donor–Acceptor Interactions and Electron Transfer in Cyano-Bridged Trinuclear Compounds. *Inorg. Chem.* **2006**, *45*, 10595–10604.
- (8) D'Alessandro, D. M.; Keene, F. R. Intervalence Charge Transfer (IVCT) in Trinuclear and Tetranuclear Complexes of Iron, Ruthenium, and Osmium. *Chem. Rev.* **2006**, *106*, 2270–2298.
- (9) Ma, X.; Hu, S.-M.; Tan, C.-H.; Zhang, Y.-F.; Zhang, X.-D.; Sheng, T.-L.; Wu, X.-T. From Antiferromagnetic to Ferromagnetic Interaction in Cyanido-Bridged Fe(III)–Ru(II)–Fe(III) Complexes by Change of the Central Diamagnetic Cyanido-Metal Geometry. *Inorg. Chem.* **2013**, *52*, 11343–11350.
- (10) Barthelme, K.; Jäger, M.; Kübel, J.; Friebe, C.; Winter, A.; Wächter, M.; Dietzek, B.; Schubert, U. S. Efficient Energy Transfer and Metal Coupling in Cyanide-Bridged Heterodinuclear Complexes Based on (Bipyridine)(terpyridine)ruthenium(II) and (Phenylpyridine)iridium(III) Complexes. *Inorg. Chem.* **2016**, *55*, 5152–5167.
- (11) Goodwin, A. L.; Kennedy, B. J.; Kepert, C. J. Thermal Expansion Matching via Framework Flexibility in Zinc Dicyanometallates. *J. Am. Chem. Soc.* **2009**, *131*, 6334–6335.
- (12) Korčok, J. L.; Katz, M. J.; Leznoff, D. B. Impact of Metallophilicity on “Colossal” Positive and Negative Thermal

Expansion in a Series of Isostructural Dicyanometallate Coordination Polymers. *J. Am. Chem. Soc.* **2009**, *131*, 4866–4871.

(13) Cairns, A. B.; Catafesta, J.; Levelut, C.; Rouquette, J.; van der Lee, A.; Peters, L.; Thompson, A. L.; Dmitriev, V.; Haines, J.; Goodwin, A. L. Giant negative linear compressibility in zinc dicyanoaurate. *Nat. Mater.* **2013**, *12*, 212–216.

(14) Ovens, J. S.; Leznoff, D. B. Thermal Expansion Behavior of $M[AuX_2(CN)_2]^-$ Based Coordination Polymers ($M = Ag, Cu; X = CN, Cl, Br$). *Inorg. Chem.* **2017**, *56*, 7332–7343.

(15) Sergeenko, A. S.; Ovens, J. S.; Leznoff, D. B. Designing anisotropic cyanometallate coordination polymers with unidirectional thermal expansion (TE): 2D zero and 1D colossal positive TE. *Chem. Commun.* **2018**, *54*, 1599–1602.

(16) Katz, M. J.; Kaluarachchi, H.; Batchelor, R. J.; Bokov, A. A.; Ye, Z.-G.; Leznoff, D. B. Highly Birefringent Materials Designed Using Coordination Polymer Synthetic Methodology. *Angew. Chem., Int. Ed.* **2007**, *46*, 8804–8807.

(17) Thompson, J. R.; Katz, M. J.; Williams, V. E.; Leznoff, D. B. Structural Design Parameters for Highly Birefringent Coordination Polymers. *Inorg. Chem.* **2015**, *54*, 6462–6471.

(18) Omary, M. A.; Patterson, H. H. Temperature-Dependent Photoluminescence Properties of $Tl[Ag(CN)_2]$: Formation of Luminescent Metal-Metal-Bonded Inorganic Exciplexes in the Solid State. *Inorg. Chem.* **1998**, *37*, 1060–1066.

(19) Lin, Y.-Y.; Lai, S.-W.; Che, C.-M.; Fu, W.-F.; Zhou, Z.-Y.; Zhu, N. Structural Variations and Spectroscopic Properties of Luminescent Mono- and Multinuclear Silver(I) and Copper(I) Complexes Bearing Phosphine and Cyanide Ligands. *Inorg. Chem.* **2005**, *44*, 1511–1524.

(20) Liu, X.; Guo, G.-C.; Fu, M.-L.; Liu, X.-H.; Wang, M.-S.; Huang, J.-S. Three Novel Silver Complexes with Ligand-Unsupported Argentophilic Interactions and Their Luminescent Properties. *Inorg. Chem.* **2006**, *45*, 3679–3685.

(21) Maynard, B. A.; Smith, P. A.; Ladner, L.; Jaleel, A.; Beedoe, N.; Crawford, C.; Assefa, Z.; Sykora, R. E. Emission Enhancement through Dual Donor Sensitization: Modulation of Structural and Spectroscopic Properties in a Series of Europium Tetracyanoplatinate. *Inorg. Chem.* **2009**, *48*, 6425–6435.

(22) Ladner, L.; Ngo, T.; Crawford, C.; Assefa, Z.; Sykora, R. E. Solid-State Photoluminescence Sensitization of Tb^{3+} by Novel Au_2Pt_2 and Au_3Pt_4 Cyanide Clusters. *Inorg. Chem.* **2011**, *50*, 2199–2206.

(23) Smith, P. A.; Crawford, C.; Beedoe, N.; Assefa, Z.; Sykora, R. E. Synthesis, Crystal Structures, and Dual Donor Luminescence Sensitization in Novel Terbium Tetracyanoplatinates. *Inorg. Chem.* **2012**, *51*, 12230–12241.

(24) Ghazzali, M.; Jaafar, M. H.; Akerboom, S.; Alsalmeh, A.; Al-Farhan, K.; Reedijk, J. A series of bimetallic chain coordination polymers bearing $[Ag(PPh_3)_2]$ chromophores: Synthesis, structure and luminescence. *Inorg. Chem. Commun.* **2013**, *36*, 18–21.

(25) Ovens, J. S.; Christensen, P. R.; Leznoff, D. B. Designing Tunable White-Light Emission from an Auophilic Cu^I/Au^I Coordination Polymer with Thioether Ligands. *Chem. - Eur. J.* **2016**, *22*, 8234–8239.

(26) Ma, F.; Gao, S.-M.; Wu, M.-M.; Zhao, J.-P.; Liu, F.-C.; Li, N.-X. An unprecedented 2D copper(I)–cyanide complex with 20-membered metal rings: the effect of the co-ligand 4,5-diazafluoren-9-one. *Dalton Trans* **2016**, *45*, 2796–2799.

(27) Roberts, R. J.; Le, D.; Leznoff, D. B. Color-Tunable and White-Light Luminescence in Lanthanide–Dicyanoaurate Coordination Polymers. *Inorg. Chem.* **2017**, *56*, 7948–7959.

(28) Belyaev, A.; Eskelinen, T.; Dau, T. M.; Ershova, Y. Y.; Tunik, S. P.; Melnikov, A. S.; Hirva, P.; Koshevoy, I. O. Cyanide-assembled d^{10} coordination polymers and cycles: excited state metallophilic modulation of solid-state luminescence. *Chem. - Eur. J.* **2018**, *24*, 1404–1415.

(29) Katz, M. J.; Ramnial, T.; Yu, H.-Z.; Leznoff, D. B. Polymorphism of $Zn[Au(CN)_2]_2$ and Its Luminescent Sensory Response to NH_3 Vapor. *J. Am. Chem. Soc.* **2008**, *130*, 10662–10673.

(30) Thomas, R. B.; Smith, P. A.; Jaleel, A.; Vogel, P.; Crawford, C.; Assefa, Z.; Sykora, R. E. Synthesis, Structural, and Photoluminescence

Studies of $Gd(terpy)(H_2O)(NO_3)_2M(CN)_2$ ($M = Au, Ag$) Complexes: Multiple Emissions from Intra- and Intermolecular Excimers and Exciplexes. *Inorg. Chem.* **2012**, *51*, 3399–3408.

(31) Yamagishi, A.; Kawasaki, T.; Hiruma, K.; Sato, H.; Kitazawa, T. Emission behaviour of a series of bimetallic $Cd(II)$ – $Au(I)$ coordination polymers. *Dalton Trans* **2016**, *45*, 7823–7828.

(32) Varju, B. R.; Ovens, J. S.; Leznoff, D. B. Mixed $Cu(I)/Au(I)$ coordination polymers as reversible turn-on vapoluminescent sensors for volatile thioethers. *Chem. Commun.* **2017**, *53*, 6500–6503.

(33) Ali, N. M.; MacLeod, V. L.; Jennison, P.; Sazanovich, I. V.; Hunter, C. A.; Weinstein, J. A.; Ward, M. D. Luminescent cyanometallates based on phenylpyridine-Ir(III) units: solvatochromism, metallochromism, and energy-transfer in Ir/Ln and Ir/Re complexes. *Dalton Trans* **2012**, *41*, 2408–2419.

(34) Ward, M. D. Structural and photophysical properties of luminescent cyanometallates $[M(\text{diimine})(CN)_4]^{2-}$ and their supramolecular assemblies. *Dalton Trans* **2010**, *39*, 8851–8867.

(35) Cadranel, A.; Oviedo, P. S.; Alborés, P.; Baraldo, L. M.; Guldi, D. M.; Hodak, J. H. Electronic Energy Transduction from $\{Ru(py)_4\}$ Chromophores to $Cr(III)$ Luminophores. *Inorg. Chem.* **2018**, *57*, 3042–3053.

(36) Kumar, A.; Sun, S.-S.; Lees, A. J. Photophysics and Photochemistry of Organometallic Rhenium Diimine Complexes. *Top. Organomet. Chem.* **2010**, *29*, 1–35.

(37) Zhao, G.-W.; Zhao, J.-H.; Hu, Y.-X.; Zhang, D.-Y.; Li, X. Recent advances of neutral rhenium(I) tricarbonyl complexes for application in organic light-emitting diodes. *Synth. Met.* **2016**, *212*, 131–141.

(38) Rohacova, J.; Ishitani, O. Photofunctional multinuclear rhenium(I) diimine carbonyl complexes. *Dalton Trans* **2017**, *46*, 8899–8919.

(39) Fredericks, S. M.; Luong, J. C.; Wrighton, M. S. Multiple Emissions from Rhenium(I) Complexes: Intraligand and Charge-Transfer Emission from Substituted Metal Carbonyl Cations. *J. Am. Chem. Soc.* **1979**, *101*, 7415–7417.

(40) Sacksteder, L.; Zipp, A. P.; Brown, E. A.; Streich, J.; Demas, J. N.; DeGraff, B. A. Luminescence Studies of Pyridine α -Diimine Rhenium(I) Tricarbonyl Complexes. *Inorg. Chem.* **1990**, *29*, 4335–4340.

(41) Casula, A.; Nairi, V.; Fernández-Moreira, V.; Laguna, A.; Lippolis, V.; Garau, A.; Gimeno, M. C. Re(I) derivatives functionalised with thioether crowns containing the 1,10-phenanthroline subunit as a new class of chemosensors. *Dalton Trans* **2015**, *44*, 18506–18517.

(42) Salignac, B.; Grundler, P. V.; Cayemittes, S.; Frey, U.; Scopelliti, R.; Merbach, A. E.; Hedinger, R.; Hegetschweiler, K.; Alberto, R.; Prinz, U.; Raabe, G.; Kölle, U.; Hall, S. Reactivity of the Organometallic $fac-[(CO)_3Re^I(H_2O)_3]^+$ Aquaion. Kinetic and Thermodynamic Properties of H_2O Substitution. *Inorg. Chem.* **2003**, *42*, 3516–3526.

(43) Chakraborty, I.; Jimenez, J.; Sameera, W. M. C.; Kato, M.; Mascharak, P. K. Luminescent Re(I) Carbonyl Complexes as Trackable PhotoCORMs for CO delivery to Cellular Targets. *Inorg. Chem.* **2017**, *56*, 2863–2873.

(44) Hormann-Arendt, A. L.; Shaw, C. F. I. Ligand-scrambling reactions of cyano(trialkyl/triarylphosphine)gold(I) complexes: examination of factors influencing the equilibrium constant. *Inorg. Chem.* **1990**, *29*, 4683–4687.

(45) APEX2 - Software Suite for Crystallographic Programs; Bruker AXS, Inc.: Madison, WI, 2010.

(46) Sheldrick, G. M. Crystal structure refinement with SHELXL. *Acta Crystallogr., Sect. C: Struct. Chem.* **2015**, *71*, 3–8.

(47) Farrugia, L. J. WinGX and ORTEP for Windows: an Update. *J. Appl. Crystallogr.* **2012**, *45*, 849–854.

(48) Sheldrick, G. M. SADABS-2008/1 - Bruker AXS Area Detector Scaling and Absorption Correction; Bruker AXS: Madison, WI, 2008.

(49) Spek, A. L. PLATON, A Multipurpose Crystallographic Tool, 1.17; Utrecht University: Utrecht, The Netherlands, 2013.

- (50) Brouwer, A. M. Standards for photoluminescence quantum yield measurements in solution (IUPAC Technical Report). *Pure Appl. Chem.* **2011**, *83*, 2213–2228.
- (51) Perdew, J. P.; Burke, K.; Ernzerhof, M. Generalized Gradient Approximation Made Simple. *Phys. Rev. Lett.* **1996**, *77*, 3865–3868.
- (52) Adamo, C.; Barone, V. Toward reliable density functional methods without adjustable parameters: The PBE0 model. *J. Chem. Phys.* **1999**, *110*, 6158–6170.
- (53) Schäfer, A.; Huber, C.; Ahlrichs, R. Fully optimized contracted Gaussian basis sets of triple zeta valence quality for atoms Li to Kr. *J. Chem. Phys.* **1994**, *100*, 5829–5835.
- (54) Eichkorn, K.; Treutler, O.; Öhm, H.; Häser, M.; Ahlrichs, R. Auxiliary basis sets to approximate Coulomb potentials. *Chem. Phys. Lett.* **1995**, *240*, 283–290.
- (55) Sierka, M.; Hogekamp, A.; Ahlrichs, R. Fast evaluation of the Coulomb potential for electron densities using multipole accelerated resolution of identity approximation. *J. Chem. Phys.* **2003**, *118*, 9136–9148.
- (56) Furche, F.; Rappoport, D. Density Functional Methods for Excited States: Equilibrium Structure and Electronic Spectra. In *Computational Photochemistry*; Olivucci, M., Ed.; Elsevier: Amsterdam, 2005; pp 93–128.
- (57) Furche, F.; Ahlrichs, R. Adiabatic time-dependent density functional methods for excited state properties. *J. Chem. Phys.* **2002**, *117*, 7433–7447.
- (58) TURBOMOLE V7.3; TURBOMOLE GmbH, 2018.
- (59) Ahlrichs, R.; Bär, M.; Häser, M.; Horn, H.; Kölmel, C. Electronic Structure Calculations on Workstation Computers: the Program System Turbomole. *Chem. Phys. Lett.* **1989**, *162*, 165–169.
- (60) Pérez, J.; Hevia, E.; Riera, L.; Riera, V.; García-Granda, S.; García-Rodríguez, E.; Miguel, D. Mono- and Dimetallic Cyano Complexes with $\{Mo(\eta^3\text{-allyl})(CO)_2(N-N)\}$ Fragments. *Eur. J. Inorg. Chem.* **2003**, *2003*, 1113–1120.
- (61) Ko, C.-C.; Ng, C.-O.; Yiu, S.-M. Luminescent Rhenium(I) Phenanthroline Complexes with a Benzoxazol-2-ylidene Ligand: Synthesis, Characterization, and Photophysical Study. *Organometallics* **2012**, *31*, 7074–7084.
- (62) Koike, K.; Tanabe, J.; Toyama, S.; Tsubaki, H.; Sakamoto, K.; Westwell, J. R.; Johnson, F. P. A.; Hori, H.; Saitoh, H.; Ishitani, O. New Synthetic Routes to Biscarbonylbipyridinerhenium(I) Complexes *cis,trans*-[Re(X₂bpy)(CO)₂(PR₃)(Y)]ⁿ⁺ (X₂bpy = 4,4'-X₂-2,2'-bipyridine) via Photochemical Ligand Substitution Reactions, and Their Photophysical and Electrochemical Properties. *Inorg. Chem.* **2000**, *39*, 2777–2783.
- (63) Tsubaki, H.; Sekine, A.; Ohashi, Y.; Koike, K.; Takeda, H.; Ishitani, O. Control of Photochemical, Photophysical, Electrochemical, and Photocatalytic Properties of Rhenium(I) Complexes Using Intramolecular Weak Interactions between Ligands. *J. Am. Chem. Soc.* **2005**, *127*, 15544–15555.
- (64) Asatani, T.; Nakagawa, Y.; Funada, Y.; Sawa, S.; Takeda, H.; Morimoto, T.; Koike, K.; Ishitani, O. Ring-Shaped Rhenium(I) Multinuclear Complexes: Improved Synthesis and Photoinduced Multielectron Accumulation. *Inorg. Chem.* **2014**, *53*, 7170–7180.
- (65) Henderson, W.; McIndoe, J. S. *Mass Spectrometry of Inorganic, Coordination and Organometallic Compounds*; Wiley: Chichester, U.K., 2005.
- (66) Isab, A. A.; Hussain, M. S.; Akhtar, M. N.; Wazeer, M. I. M.; Al-Arfaj, A. R. ¹³C, ¹⁵N and ³¹P NMR study of the disproportionation of cyanogold(I) complexes: [R₃PAu¹³C¹⁵N]. *Polyhedron* **1999**, *18*, 1401–1409.
- (67) Raab, K.; Beck, W. Metallorganische Lewis-Säuren, XVI. Reaktionen von Pentacarbonyl(tetrafluoroborato)rhenium(I) mit einfachen und komplexen Anionen. *Chem. Ber.* **1985**, *118*, 3830–3848.
- (68) Hartmann, H.; Kaim, W.; Wanner, M.; Klein, A.; Frantz, S.; Duboc-Toia, C.; Fiedler, J.; Zálaiš, S. Proof of Innocence for the Quintessential Noninnocent Ligand TCNQ in Its Tetranuclear Complex with Four [fac-Re(CO)₃(bpy)]⁺ Groups: Unusually Different Reactivity of the TCNX Ligands (TCNX = TCNE, TCNQ, TCNB). *Inorg. Chem.* **2003**, *42*, 7018–7025.
- (69) Parker, R. J.; Hockless, D. C. R.; Moubarki, B.; Murray, K. S.; Spiccia, L. Hexacyanometalates as templates for heteropolynuclear complexes and molecular magnets: synthesis and crystal structure of [Fe{(CN)Cu(tpa)}₆][ClO₄]₈·3H₂O, [tpa = tris(2-pyridylmethyl)-amine]. *Chem. Commun.* **1996**, 2789–2790.
- (70) Flay, M.-L.; Vahrenkamp, H. Cyanide-Bridged Oligonuclear Complexes Containing Ni-CN-Cu and Pt-CN-Cu Linkages. *Eur. J. Inorg. Chem.* **2003**, *2003*, 1719–1726.
- (71) Shen, X.; Li, B.; Zou, J.; Hu, H.; Xu, Z. The first cyano-bridged heptanuclear Mn(III)6Fe(III) cluster: crystal structure and magnetic properties of [Mn(salen)·H₂O]6Fe(CN)₆[Fe(CN)₆]·6H₂O. *J. Mol. Struct.* **2003**, *657*, 325–331.
- (72) Maxim, C.; Sorace, L.; Khuntia, P.; Madalan, A. M.; Kravtsov, V.; Lascialfari, A.; Caneschi, A.; Journaux, Y.; Andruh, M. A missing high-spin molecule in the family of cyanido-bridged heptanuclear heterometal complexes, [(LCu^{II})₆Fe^{III}(CN)₆]³⁺, and its Co^{III} and Cr^{III} analogues, accompanied in the crystal by a novel octameric water cluster. *Dalton Trans* **2010**, *39*, 4838–4847.
- (73) Wallace, L.; Rillema, D. P. Photophysical Properties of Rhenium(I) Tricarbonyl Complexes Containing Alkyl- and Aryl-Substituted Phenanthrolines as Ligands. *Inorg. Chem.* **1993**, *32*, 3836–3843.
- (74) Fernández-Moreira, V.; Marzo, I.; Gimeno, M. C. Luminescent Re(I) and Re(I)/Au(I) complexes as cooperative partners in cell imaging and cancer therapy. *Chem. Sci.* **2014**, *5*, 4434–4446.
- (75) Chu, W.-K.; Wei, X.-G.; Yiu, S.-M.; Ko, C.-C.; Lau, K.-C. Strongly Phosphorescent Neutral Rhenium(I) Isocyanoborato Complexes: Synthesis, Characterization, and Photophysical, Electrochemical, and Computational Studies. *Chem. - Eur. J.* **2015**, *21*, 2603–2612.
- (76) Ko, C.-C.; Cheung, A. W.-Y.; Yiu, S.-M. Synthesis, photophysical and electrochemical study of diisocyno-bridged homodinuclear rhenium(I) diimine complexes. *Polyhedron* **2015**, *86*, 17–23.
- (77) Rohacova, J.; Sekine, A.; Kawano, T.; Tamari, S.; Ishitani, O. Trinuclear and Tetranuclear Re(I) Rings Connected with Phenylene, Vinylene, and Ethynylene Chains: Synthesis, Photophysics, and Redox Properties. *Inorg. Chem.* **2015**, *54*, 8769–8777.
- (78) Tso-Lun Lo, L.; Lai, S.-W.; Yiu, S.-M.; Ko, C.-C. A new class of highly solvatochromic dicyano rhenate(I) diimine complexes – synthesis, photophysics and photocatalysis. *Chem. Commun.* **2013**, *49*, 2311–2313.
- (79) Kurtz, D. A.; Brereton, K. R.; Ruoff, K. P.; Tang, H. M.; Felton, G. A. N.; Miller, A. J. M.; Dempsey, J. L. Bathochromic Shifts in Rhenium Carbonyl Dyes Induced through Destabilization of Occupied Orbitals. *Inorg. Chem.* **2018**, *57*, 5389–5399.
- (80) Lever, A. B. P. *Inorganic Electronic Spectroscopy*, 2nd ed.; Elsevier: Amsterdam, 1984.
- (81) Wrighton, M.; Morse, D. L. The Nature of the Lowest Excited State in Tricarbonylchloro-1,10-phenanthrolinerhenium(I) and Related Complexes. *J. Am. Chem. Soc.* **1974**, *96*, 998–1003.
- (82) Worl, L. A.; Duesing, R.; Chen, P.; Della Ciana, L.; Meyer, T. J. Photophysical properties of polypyridyl carbonyl complexes of rhenium(I). *J. Chem. Soc., Dalton Trans.* **1991**, 849–858.
- (83) Takeda, H.; Koike, K.; Inoue, H.; Ishitani, O. Development of an Efficient Photocatalytic System for CO₂ Reduction Using Rhenium(I) Complexes Based on Mechanistic Studies. *J. Am. Chem. Soc.* **2008**, *130*, 2023–2031.
- (84) Moore, S. A.; Frazier, S. M.; Sibbald, M. S.; DeGraff, B. A.; Demas, J. N. On the Causes of Altered Photophysics of Luminescent Metal Complexes Embedded in Polymer Hosts. *Langmuir* **2011**, *27*, 9567–9575.
- (85) Kalyanasundaram, K. Luminescence and redox reactions of the metal-to-ligand charge-transfer excited state of tricarbonylchloro-(polypyridyl)rhenium(I) complexes. *J. Chem. Soc., Faraday Trans. 2* **1986**, *82*, 2401–2415.
- (86) Polo, A. S.; Itokazu, M. K.; Frin, K. M.; de Toledo Patrocínio, A. O.; Murakami Iha, N. Y. Light driven trans-to-cis isomerization of

stilbene-like ligands in $\text{fac-}[\text{Re}(\text{CO})_3(\text{NN})(\text{trans-L})]^+$ and luminescence of their photoproducts. *Coord. Chem. Rev.* **2006**, *250*, 1669–1680.

(87) Werrett, M. V.; Chartrand, D.; Gale, J. D.; Hanan, G. S.; MacLellan, J. G.; Massi, M.; Muzzioli, S.; Raiteri, P.; Skelton, B. W.; Silberstein, M.; Stagni, S. Synthesis, Structural, and Photophysical Investigation of Diimine Tricarbonyl Re(I) Tetrazolato Complexes. *Inorg. Chem.* **2011**, *50*, 1229–1241.

(88) Caspar, J. V.; Meyer, T. J. Application of the energy gap law to nonradiative, excited-state decay. *J. Phys. Chem.* **1983**, *87*, 952–957.

(89) Hallett, A. J.; Pope, S. J. A. Towards near-IR emissive rhenium tricarbonyl complexes: Synthesis and characterisation of unusual 2,2'-biquinoline complexes. *Inorg. Chem. Commun.* **2011**, *14*, 1606–1608.

(90) McLean, T. M.; Moody, J. L.; Waterland, M. R.; Telfer, S. G. Luminescent Rhenium(I)-Dipyrrinato Complexes. *Inorg. Chem.* **2012**, *51*, 446–455.

(91) Yu, T.; Tsang, D. P.-K.; Au, V. K.-M.; Lam, W. H.; Chan, M.-Y.; Yam, V. W.-W. Deep Red to Near-Infrared Emitting Rhenium(I) Complexes: Synthesis, Characterization, Electrochemistry, Photo-physics, and Electroluminescence Studies. *Chem. - Eur. J.* **2013**, *19*, 13418–13427.

(92) Wrighton, M.; Morse, D. L. Nature of the Lowest Excited State in Tricarbonylchloro-1,10-phenanthroline-rhenium(I) and Related Complexes. *J. Am. Chem. Soc.* **1974**, *96*, 998–1003.

(93) Kotch, T. G.; Lees, A. J.; Fuerniss, S. J.; Papatomas, K. I.; Snyder, R. W. Luminescence Rigidochromism of $\text{fac-ClRe}(\text{CO})_3(4,7\text{-Ph}_2\text{phen})$ ($4,7\text{-Ph}_2\text{phen} = 4,7\text{-Diphenyl-1,10-phenanthroline}$) as a Spectroscopic Probe in Monitoring Polymerization of Photosensitive Thin Films. *Inorg. Chem.* **1993**, *32*, 2570–2575.

(94) Itokazu, M. K.; Polo, A. S.; Iha, N. Y. M. Luminescent rigidochromism of $\text{fac-}[\text{Re}(\text{CO})_3(\text{phen})(\text{cis-bpe})]^+$ and its binuclear complex as photosensor. *J. Photochem. Photobiol., A* **2003**, *160*, 27–32.

(95) Cheung, K.-L.; Yip, S.-K.; Yam, V. W.-W. Synthesis, characterization, electrochemistry and luminescence studies of heterometallic gold(I)–rhenium(I) alkynyl complexes. *J. Organomet. Chem.* **2004**, *689*, 4451–4462.

(96) Scholz, F.; Schröder, U.; Gulabowski, R.; Doménech-Carbó, A. *Electrochemistry of Immobilized Particles and Droplets*, 2nd ed.; Springer: Berlin-Heidelberg, 2015.

(97) Doménech-Carbó, A.; Labuda, J.; Scholz, F. Electroanalytical chemistry for the analysis of solids: Characterization and classification. *Pure Appl. Chem.* **2012**, *85*, 609–631.

(98) Doménech, A.; Koshevoy, I. O.; Montoya, N.; Pakkanen, T. A. Electrochemically assisted anion insertion in Au(I)-Cu(I) hetero-trimetallic clusters bearing ferrocenyl groups: Application to the Fluoride/Chloride discrimination in aqueous media. *Electrochem. Commun.* **2010**, *12*, 206–209.

(99) Doménech-Carbó, A.; Koshevoy, I.; Montoya, N.; Pakkanen, T. A.; Doménech-Carbó, M. T. Solvent-Independent Electrode Potentials of Solids Undergoing Insertion Electrochemical Reactions: Part II. Experimental Data for Alkynyl-Diphosphine Dinuclear Au(I) complexes Undergoing Electron Exchange Coupled to Anion Exchange. *J. Phys. Chem. C* **2012**, *116*, 25984–25992.

(100) Gonçalves, M. R.; Frin, K. P. M. Synthesis, characterization, photophysical and electrochemical properties of $\text{fac-tricarbonyl}(4,7\text{-dichloro-1,10-phenanthroline})\text{rhenium(I)}$ complexes. *Polyhedron* **2015**, *97*, 112–117.

(101) Gutmann, V.; Gritzner, G.; Danksagmüller, K. Solvent effects on the redox potential of hexacyanoferrate(III)-Hexacyanoferrate(II). *Inorg. Chim. Acta* **1976**, *17*, 81–86.